

# Community Detection and Classification in Hierarchical Stochastic Blockmodels

Vince Lyzinski, Minh Tang, Avanti Athreya, Youngser Park, Carey E. Priebe

**Abstract**—In disciplines as diverse as social network analysis and neuroscience, many large graphs are believed to be composed of loosely connected smaller graph primitives, whose structure is more amenable to analysis. We propose a robust, scalable, integrated methodology for *community detection* and *community comparison* in graphs. In our procedure, we first embed a graph into an appropriate Euclidean space to obtain a low-dimensional representation, and then cluster the vertices into communities. We next employ nonparametric graph inference techniques to identify structural similarity among these communities. These two steps are then applied recursively on the communities, allowing us to detect more fine-grained structure. We describe a *hierarchical stochastic blockmodel*—namely, a stochastic blockmodel with a natural hierarchical structure—and establish conditions under which our algorithm yields consistent estimates of model parameters and *motifs*, which we define to be stochastically similar groups of subgraphs. Finally, we demonstrate the effectiveness of our algorithm in both simulated and real data. Specifically, we address the problem of locating similar sub-communities in a partially reconstructed *Drosophila* connectome and in the social network Friendster.



## 1 INTRODUCTION

The representation of data as graphs, with the vertices as entities and the edges as relationships between the entities, is now ubiquitous in many application domains: for example, social networks, in which vertices represent individual actors or organizations [1]; neuroscience, in which vertices are neurons or brain regions [2]; and document analysis, in which vertices represent authors or documents [3]. This representation has proven invaluable in describing and modeling the intrinsic and complex structure that underlies these data.

In understanding the structure of large, complex graphs, a central task is that of identifying and classifying local, lower-dimensional structure, and more specifically, consistently and scalably estimating subgraphs and sub-communities. In disciplines as diverse as social network analysis and neuroscience, many large graphs are believed to be composed of loosely connected smaller graph primitives, whose structure is more amenable to analysis. For example, the widely-studied social network Friendster<sup>1</sup>, which has approximately 60 million users and 2 billion edges, is believed to consist of over 1 million communities at local-scale. Inasmuch as the communication structure of these social communities both influences and is influenced by the function of the social community, we expect there to be repeated structure across many of these communities (see Section 5). As a second motivating example, the neuroscientific *cortical column conjecture* [4, 5] posits that the neocortex of the human brain employs algorithms composed of repeated instances of a limited set of computing primitives. By

modeling certain portions of the cortex as a hierarchical random graph, the cortical column conjecture can be interpreted as a problem of community detection and classification within a graph. While the full data needed to test the cortical column conjecture is not yet available [6], it nonetheless motivates our present approach of theoretically-sound robust hierarchical community detection and community classification.

Community detection for graphs is a well-established field of study, and there are many techniques and methodologies available, such as those based on maximizing modularity and likelihood [7, 8, 9], random walks [10, 11], and spectral clustering and partitioning [12, 13, 14, 15, 16, 17]. While many of these results focus on the consistency of the algorithms—namely, that the proportion of misclassified vertices goes to zero—the key results in this paper give guarantees on the probability of *perfect clustering*, in which no vertices at all are misclassified. As such, they are similar in spirit to the results of [7] and represent a considerable improvement of our earlier clustering results from [18]. As might be expected, though, the strength of our results depends on the average degree of the graph, which we require to grow at least at order  $\sqrt{n} \log^2(n)$ . We note that weak or partial recovery results are available for much sparser regimes, e.g., when the average degree stays bounded as the number of vertices  $n$  increases (see, for example, the work of [19]). A partial summary of various consistency results and sparsity regimes in which they hold is given in Table 1. Existing theoretical results on clustering have also been centered primarily on isolating fine-grained community structure in a network. A major contribution of this work, then, is a formal delineation of *hierarchical* structure in a network and a provably consistent algorithm to uncover communities and subgraphs at multiple scales.

Moreover, existing community detection algorithms

• V.L. is with Johns Hopkins University Human Language Technology Center of Excellence. M. T., A. A. and C. E. P. are with Johns Hopkins University Department of Applied Mathematics and Statistics. Y. P. is with Johns Hopkins University Center for Imaging Sciences. .

1. available from <http://snap.stanford.edu/data>

Average degree	Method	Notion of recovery	References
$O(1)$	semidefinite programming, backtracking random walks	weak recovery	[19, 20, 21]
$\Omega(\log n)$	spectral clustering	weak consistency	[13, 14, 22]
$\Omega(\log n)$	modularity maximization	strong consistency	[7]
$\Omega(\sqrt{n} \log^2 n)$	spectral clustering	strong consistency	[18]

TABLE 1: A summary of some existing results on the consistency of recovering the block assignments in stochastic blockmodel graphs with fixed number of blocks. Weak recovery and weak consistency correspond to the notions that, in the limit as  $n \rightarrow \infty$ , the proportion of correctly classified vertices is non-zero and approaches one in probability, respectively. Strong consistency corresponds to the notion that the number of misclassified vertices is zero in the limit.

have focused mostly on uncovering the subgraphs. Recently, however, the characterization and classification of these subgraphs into stochastically similar motifs has emerged as an important area of ongoing research. Network comparison is a nascent field, and comparatively few techniques have thus far been proposed; see [23, 24, 25, 26, 27, 28, 29]. In particular, in [28], the authors exhibit a consistent nonparametric test for the equality of two generating distributions for a pair of random graphs. The method is based on first embedding the networks into Euclidean space followed by computing  $L_2$  distances between the density estimates of the resulting embeddings. This hypothesis test will play a central role in our present methodology; see Section 2.

In the present paper, we introduce a robust, scalable methodology for *community detection* and *community comparison* in graphs, with particular application to social networks and connectomics. Our techniques build upon previous work in graph embedding, parameter estimation, and multi-sample hypothesis testing (see [14, 18, 28, 29]). Our method proceeds as follows. First, we generate a low-dimensional representation of the graph [14], cluster to detect subgraphs of interest [18], and then employ the nonparametric inference techniques of [28] to identify heterogeneous subgraph structures. The representation of a network as a collection of points in Euclidean space allows for a single framework which combines the steps of community detection via an adapted spectral clustering procedure (Algorithm 2) with network comparison via density estimation. Indeed, the streamlined clustering algorithm proposed in this paper, Algorithm 2, is well-suited to our hierarchical framework, whereas classical  $K$ -means may be ill-suited to the pathologies of this model. As a consequence, we are able to present in this paper a unified inference procedure in which community detection, motif identification, and larger network comparison are all seamlessly integrated.

We focus here on a *hierarchical* version of the classical stochastic block model [30, 31], in which the larger graph is comprised of smaller subgraphs, each themselves approximately stochastic blockmodels. We emphasize that our model and subsequent theory rely heavily on an affinity assumption at each level of the hierarchy, and we expect our model to be a reasonable surrogate for a wide range of real networks, as corroborated by our empirical

results. In our approach, we aim to infer finer-grained structure at each level of our hierarchy, in effect performing a “top-down” decomposition. (For a different generative hierarchical model, in which successive-level blocks and memberships are the inference tasks, see [32].) We recall that the stochastic blockmodel (SBM) is an independent-edge random graph model that posits that the probability of connection between any two vertices is a function of the *block memberships* (i.e., community memberships) of the vertices. As such, the stochastic blockmodel is commonly used to model community structure in graphs. While we establish performance guarantees for this methodology in the setting of hierarchical stochastic blockmodels (HSBM), we demonstrate the wider effectiveness of our algorithm for simultaneous community detection and classification in the *Drosophila* connectome and the very-large scale social network Friendster, which has approximately 60 million users and 2 billion edges.

We organize the paper as follows. In Section 2, we provide the key definitions in our model, specifically for random dot product graphs, SBM graphs, and HSBM graphs. We summarize recent results on networks comparison from [28], which is critical to our main algorithm, Algorithm 1. We also present our novel clustering procedure, Algorithm 2. In Section 3, we demonstrate how, under mild model assumptions, Algorithm 1 can be applied to asymptotically almost surely perfectly recover the motif structure in a two-level HSBM, see Theorem 9. In Section 4, we consider a HSBM with multiple levels and discuss the recursive nature of Algorithm 1. We also extend Theorem 9 to the multi-level HSBM and show, under mild model assumptions, Algorithm 1 again asymptotically almost surely perfectly recovers the hierarchical motif structure in a multi-level HSBM. In Section 5, we demonstrate that Algorithm 1 can be effective in uncovering statistically similar subgraph structure in real data: first, in the *Drosophila* connectome, in which we uncover two repeated motifs; and second, in the Friendster social network, in which we decompose the massive network into 15 large subgraphs, each with hundreds of thousands to millions of vertices. We identify motifs among these Friendster subgraphs, and we compare two subgraphs belonging to different motifs. We further analyze a particular subgraph from a single motif and demonstrate that we can identify

structure at the second (lower) level. In Section 6, we conclude by remarking on refinements and extensions of this approach to community detection.

## 2 BACKGROUND

We situate our approach in the context of hierarchical stochastic blockmodel graphs. We first define the stochastic blockmodel as a special case of the more general random dot product graph model [33], which is itself a special case of the more general latent position random graph [34]. We next describe our canonical *hierarchical stochastic blockmodel*, which is a stochastic blockmodel that is endowed with a natural hierarchical structure.

**Notation:** In what follows, for a matrix  $M \in \mathbb{R}^{n \times m}$ , we shall use the notation  $M(i, :)$  to denote the  $i$ -th row of  $M$ , and  $M(:, i)$  to denote the  $i$ -th column of  $M$ . For a symmetric matrix  $M \in \mathbb{R}^{n \times n}$ , we shall denote the (ordered) spectrum of  $M$  via  $\lambda_1(M) \geq \lambda_2(M) \geq \dots \geq \lambda_n(M)$ .

We begin by defining the *random dot product* graph.

**Definition 1** ( $d$ -dimensional Random Dot Product Graph (RDPG)). Let  $F$  be a distribution on a set  $\mathcal{X} \subset \mathbb{R}^d$  such that  $\langle x, x' \rangle \in [0, 1]$  for all  $x, x' \in \mathcal{X}$ . We say that  $(X, A) \sim \text{RDPG}(F)$  is an instance of a random dot product graph (RDPG) if  $X = [X_1, \dots, X_n]^\top$  with  $X_1, X_2, \dots, X_n \stackrel{\text{i.i.d.}}{\sim} F$ , and  $A \in \{0, 1\}^{n \times n}$  is a symmetric hollow matrix satisfying

$$\mathbb{P}[A|X] = \prod_{i>j} (X_i^\top X_j)^{A_{ij}} (1 - X_i^\top X_j)^{1-A_{ij}}.$$

**Remark 1.** We note that non-identifiability is an intrinsic property of random dot product graphs. Indeed, for any matrix  $X$  and any orthogonal matrix  $W$ , the inner product between any rows  $i, j$  of  $X$  is identical to that between the rows  $i, j$  of  $XW$ . Hence, for any probability distribution  $F$  on  $\mathcal{X}$  and unitary operator  $U$ , the adjacency matrices  $A \sim \text{RDPG}(F)$  and  $B \sim \text{RDPG}(F \circ U)$  are identically distributed.

We denote the second moment matrix for the vectors  $X_i$  by  $\Delta = \mathbb{E}(X_1 X_1^\top)$ ; we assume that  $\Delta$  is rank  $d$ .

The stochastic blockmodel can be framed in the context of random dot product graphs as follows.

**Definition 2.** We say that an  $n$  vertex graph  $(X, A) \sim \text{RDPG}(F)$  is a (positive semidefinite) stochastic blockmodel (SBM) with  $K$  blocks if the distribution  $F$  is a mixture of  $K$  point masses,

$$F = \sum_{i=1}^K \pi(i) \delta_{\xi_i},$$

where  $\vec{\pi} \in (0, 1)^K$  satisfies  $\sum_i \pi(i) = 1$ , and the distinct latent positions are given by  $\xi = [\xi_1, \xi_2, \dots, \xi_K]^\top \in \mathbb{R}^{K \times d}$ . In this case, we write  $G \sim \text{SBM}(n, \vec{\pi}, \xi \xi^\top)$ , and we refer to  $\xi \xi^\top \in \mathbb{R}^{K, K}$  as the *block probability matrix* of  $G$ .

Moreover, any stochastic blockmodel graphs where the block probability matrix  $B$  is positive semidefinite can be formulated as a random dot product graphs where the point masses are the rows of  $B^{1/2}$ .

Many real data networks exhibit hierarchical community structure (for social network examples, see [32, 35, 36, 37, 38, 39, 40]; for biological examples, see [4, 5, 6]). To incorporate hierarchical structure into the above RDPG and SBM framework, we first consider SBM graphs endowed with the following specific hierarchical structure.

**Definition 3** (2-level Hierarchical stochastic blockmodel (HSBM)). We say that  $(X, A) \sim \text{RDPG}(F)$  is an instantiation of a  $D$ -dimensional 2-level hierarchical stochastic blockmodel with parameters  $(n, \vec{\pi}, \{\vec{\pi}_i\}_{i=1}^R, \xi)$  if  $F$  can be written as the mixture

$$F = \sum_{i=1}^R \pi(i) F_i,$$

where  $\vec{\pi} \in (0, 1)^R$  satisfies  $\sum_i \pi(i) = 1$ , and for each  $i \in [R]$ ,  $F_i$  is itself a mixture of point mass distributions

$$F_i = \sum_{j=1}^{K_i} \pi_i(j) \delta_{\xi_i^{(j)}(\cdot, j)}$$

where  $\vec{\pi}_i \in (0, 1)^{K_i}$  satisfies  $\sum_j \pi_i(j) = 1$ . The distinct latent positions are then given by  $\xi = [\xi_1^{(2)} | \dots | \xi_R^{(2)}]^\top \in \mathbb{R}^{(\sum_i K_i) \times D}$ . We then write

$$G \sim \text{HSBM}(n, \vec{\pi}, \{\vec{\pi}_i\}_{i=1}^R, \xi \xi^\top).$$

Simply stated, an HSBM graph is an RDPG for which the vertex set can be partitioned into  $R$  subgraphs—where  $(\xi_i^{(2)})^\top \in \mathbb{R}^{K_i \times D}$  denotes the matrix whose rows are the latent positions characterizing the block probability matrix for subgraph  $i$ —each of which is itself an SBM.

Throughout this manuscript, we will make a number of simplifying assumptions on the underlying HSBM in order to facilitate theoretical developments and ease exposition.

**Assumption 1.** (Affinity HSBM) We further assume that for the distinct latent positions, if we define

$$q := \min_{i, h, l} \langle \xi_i^{(2)}(\cdot, l), \xi_i^{(2)}(\cdot, h) \rangle; \quad (1)$$

$$p := \max_{i \neq j} \max_{\ell, h} \langle \xi_i^{(2)}(\cdot, \ell), \xi_j^{(2)}(\cdot, h) \rangle \quad (2)$$

then  $p < q$ . Simply stated, we require that within each subgraph, the connections are comparatively dense, and between two subgraphs, comparatively sparse.

**Assumption 2.** (Subspace structure) To simplify exposition, and to assure the condition that  $\langle \xi_i^{(2)}(\cdot, \ell), \xi_j^{(2)}(\cdot, h) \rangle \leq p$  for  $1 \leq i \neq j \leq R$  and  $\ell, h \in [K]$ , we impose additional structure on the matrix of latent positions in

the HSBM. To wit, we write  $\xi \in \mathbb{R}^{RK \times D}$  explicitly as

$$\xi = \begin{bmatrix} (\xi_1^{(2)})^T \\ (\xi_2^{(2)})^T \\ \vdots \\ (\xi_R^{(2)})^T \end{bmatrix} = \underbrace{\begin{bmatrix} \xi_1^T & 0 & \cdots & 0 \\ 0 & \xi_2^T & \cdots & 0 \\ \vdots & \vdots & \ddots & \vdots \\ 0 & 0 & \cdots & \xi_R^T \end{bmatrix}}_{Z^{(2)}} + \mathcal{A}^{(2)},$$

where  $Z^{(2)} \circ \mathcal{A}^{(2)} = 0$  ( $\circ$  being the Hadamard product) and the entries of  $\mathcal{A}^{(2)}$  are chosen to make the off block-diagonal elements of the corresponding edge probability matrix  $\xi\xi^T$  bounded above by the absolute constant  $p$ . Moreover, to ease exposition in this 2-level setting, we will assume that for each  $i \in [R]$ ,  $\xi_i \in \mathbb{R}^{K \times d}$  so that  $D = Rd$ . In practice, the subspaces pertaining to the individual subgraphs need not be the same rank, and the subgraphs need not have the same number of blocks (see Section 5 for examples of  $K$  and  $d$  varying across subgraphs).

**Remark 2.** Note that  $G \sim \text{HSBM}(n, \vec{\pi}, \{\vec{\pi}_i\}_{i=1}^R, \xi\xi^T)$  can be viewed as a SBM graph with  $\sum_i K_i$  blocks;  $G \sim \text{SBM}(n, (\pi(1)\vec{\pi}_1, \pi(2)\vec{\pi}_2, \dots, \pi(R)\vec{\pi}_R), \xi\xi^T)$ . However, in this paper we will consider blockmodels with statistically similar subgraphs across blocks, and in general, such models can be parameterized by far fewer than  $\sum_i K_i$  blocks. In contrast, when the graph is viewed as an RDPG, the full  $\sum_i K_i$  dimensions may be needed, because our affinity assumption necessitates a growing number of dimensions to accommodate the potentially growing number of subgraphs. Because latent positions associated to vertices in different subgraphs must exhibit near orthogonality, teasing out the maximum possible number of subgraphs for a given embedding dimension is, in essence, a cone-packing problem; while undoubtedly of interest, we do not pursue this problem further in this manuscript.

Given a graph from this model satisfying Assumptions 1 and 2, we use Algorithm 1 to uncover the hidden hierarchical structure. Furthermore, we note that Algorithm 1 can be applied to uncover hierarchical structure in any hierarchical network, regardless of HSBM model assumptions. However, our theoretical contributions are proven under HSBM model assumptions.

A key component of this algorithm is the computation of the adjacency spectral embedding [14], defined as follows.

**Definition 4.** Given an adjacency matrix  $A \in \{0, 1\}^{n \times n}$  of a  $d$ -dimensional RDPG( $F$ ), the *adjacency spectral embedding* (ASE) of  $A$  into  $\mathbb{R}^d$  is given by  $\widehat{X} = U_A S_A^{1/2}$  where

$$|A| = [U_A | \tilde{U}_A] [S_A \oplus \tilde{S}_A] [U_A | \tilde{U}_A]$$

is the spectral decomposition of  $|A| = (A^T A)^{1/2}$ ,  $S_A$  is the diagonal matrix with the (ordered)  $d$  largest eigenvalues of  $|A|$  on its diagonal, and  $U_A \in \mathbb{R}^{n \times d}$  is the matrix whose columns are the corresponding orthonormal eigenvectors of  $|A|$ .

---

### Algorithm 1 Detecting hierarchical structure for graphs

---

**Input:** Adjacency matrix  $A \in \{0, 1\}^{n \times n}$  for a latent position random graph.

**Output:** Subgraphs and characterization of their dissimilarity

**while** Cluster size exceeds threshold **do**

  Step 1: Compute the adjacency spectral embedding (see Definition 4)  $\widehat{X}$  of  $A$  into  $\mathbb{R}^D$ ;

  Step 2: Cluster  $\widehat{X}$  to obtain subgraphs  $\widehat{H}_1, \dots, \widehat{H}_R$  using the procedure described in Algorithm 2

  Step 3: For each  $i \in [R]$ , compute the adjacency spectral embedding for each subgraph  $\widehat{H}_i$  into  $\mathbb{R}^d$ , obtaining  $\widehat{X}_{\widehat{H}_i}$ ;

  Step 4: Compute  $\widehat{S} := [T_{\widehat{n}_r, \widehat{n}_s}(\widehat{X}_{\widehat{H}_r}, \widehat{X}_{\widehat{H}_s})]$ , where  $T$  is the test statistic in Theorem 8, producing a pairwise dissimilarity matrix on induced subgraphs;

  Step 5: Cluster induced subgraphs into motifs using the dissimilarities given in  $\widehat{S}$ ; e.g., use a hierarchical clustering algorithm to cluster the rows of  $\widehat{S}$  or the matrix of associated  $p$ -values.

  Step 6: Recurse on a representative subgraph from each motif (e.g., the largest subgraph), embedding into  $\mathbb{R}^d$  in Step 1 (not  $\mathbb{R}^D$ );

**end while**

---

It is proved in [14, 41] that the adjacency spectral embedding provides a consistent estimate of the true latent positions in random dot product graphs. The key to this result is a tight concentration, in Frobenius norm, of the adjacency spectral embedding,  $\widehat{X}$ , about the true latent positions  $X$ . This bound is strengthened in [18], wherein the authors show tight concentration, in  $2 \mapsto \infty$  norm, of  $\widehat{X}$  about  $X$ . The  $2 \mapsto \infty$  concentration provides a significant improvement over results that employ bounds on the Frobenius norm of the residuals between the estimated and true latent positions, namely  $\|\widehat{X} - X\|_F$ . The Frobenius norm bounds are potentially sub-optimal for subsequent inference, because one cannot rule out that a diminishing but positive proportion of the embedded points contribute disproportionately to the global error.

However, the  $2 \mapsto \infty$  norm concentration result in [18] relies on the assumption that the eigenvalues of  $\mathbb{E}[X_1 X_1^T]$  are distinct, which is often violated in the setting of repeated motifs for an HSBM. One of the main contributions of this paper is a further strengthening of the results of [18]: in Theorem 5, we prove that  $\widehat{X}$  concentrates about  $X$  in  $2 \mapsto \infty$  norm with far less restrictive assumptions on the eigenstructure of  $\mathbb{E}[X_1 X_1^T]$ .

In this paper, if  $E_n$  is a sequence of events, we say that  $E_n$  occurs asymptotically almost surely if  $P(E_n) \rightarrow 1$  as  $n \rightarrow \infty$ ; more precisely, we say that  $E_n$  occurs asymptotically almost surely if for any fixed  $c > 0$ , there exists  $n_0(c)$  such that if  $n > n_0(c)$  and  $\eta$  satisfies  $n^{-c} < \eta < 1/2$ , then  $P(E_n)$  is at least  $1 - \eta$ . The theorem below asserts that the  $2 \mapsto \infty$  norm of the

differences between true and estimated latent positions is of a certain order asymptotically almost surely. In the appendix, we state and prove a generalization of this result in the non-dense regime.

**Theorem 5.** *Let  $(A, X) \sim \text{RDPG}(F)$  where the second moment matrix  $\Delta = \mathbb{E}(X_1 X_1^T)$  is of rank  $d$ . Let  $E_n$  be the event that there exists a rotation matrix  $W$  such that*

$$\|\hat{X} - XW\|_{2 \rightarrow \infty} = \max_i \|\hat{X}(i, \cdot) - WX(i, \cdot)\| \leq \frac{Cd^{1/2} \log^2 n}{\sqrt{n}}$$

where  $C$  is some fixed constant. Then  $E_n$  occurs asymptotically almost surely.

We stress that because of this bound on the  $2 \rightarrow \infty$  norm, we have far greater control of the errors in individual rows of the residuals  $\hat{X} - X$  than possible with existing Frobenius norm bounds. One consequence of this control is that an asymptotically perfect clustering procedure for  $X$  will yield an equivalent asymptotically almost surely perfect clustering of  $\hat{X}$ . This insight is the key to proving Lemma 6, see the appendix for full detail. A further consequence of Theorem 5, in the setting of random dot product graphs without a canonical block structure, is that one can choose a loss function with respect to which ASE followed by a suitable clustering yields optimal clusters [18, 41]. This implies that meaningful clustering can be pursued even when no canonical hierarchical structure exists.

Having successfully embedded the graph  $G$  into  $\mathbb{R}^D$  through the adjacency spectral embedding, we next cluster the vertices of  $G$ , i.e., rows of  $\hat{X}$ . For each  $i \in [R]$ , we define

$$(\hat{\xi}_i^{(2)})^T \in \mathbb{R}^{|V(H_i)| \times D}$$

to be the matrix whose rows are the rows in  $\hat{X}$  corresponding to the latent positions in the rows of  $(\hat{\xi}_i^{(2)})^T$ . Our clustering algorithm proceeds as follows. With Assumptions 1 and 2, and further assuming that  $R$  is known, we first build a “seed” set  $\mathcal{S}_n$  as follows. Initialize  $\mathcal{S}_0$  to be a random sampling of  $R$  rows of  $\hat{X}$ . For each  $i \in [n]$ , let  $\tilde{y}, \tilde{z} \in \mathcal{S}_{i-1}$  be such that

$$\max_{y, z \in \mathcal{S}_{i-1}} \langle y, z \rangle = \langle \tilde{y}, \tilde{z} \rangle.$$

If  $\max_{x \in \mathcal{S}_{i-1}} \langle \hat{X}(i, \cdot), x \rangle < \langle \tilde{y}, \tilde{z} \rangle$ , then add  $\hat{X}(i, \cdot)$  to  $\mathcal{S}_{i-1}$ , and remove  $\tilde{z}$  from  $\mathcal{S}_{i-1}$ ; i.e.,

$$\mathcal{S}_i = (\mathcal{S}_{i-1} \setminus \{\tilde{z}\}) \cup \{\hat{X}(i, \cdot)\}.$$

If  $\max_{x \in \mathcal{S}_{i-1}} \langle \hat{X}(i, \cdot), x \rangle \geq \langle \tilde{y}, \tilde{z} \rangle$ , then set  $\mathcal{S}_i = \mathcal{S}_{i-1}$ . Iterate this procedure until all  $n$  rows of  $\hat{X}$  have been considered. We show in Proposition 19 in the appendix that  $\mathcal{S}_n$  is composed of exactly one row from each  $\hat{\xi}^{(i)}$ . Given the seed set  $\mathcal{S}_n = \{s_1, s_2, \dots, s_R\}$ , we then initialize  $R$  clusters  $\hat{C}_1, \hat{C}_2, \dots, \hat{C}_R$  via  $\hat{C}_i = \{s_i\}$  for each  $i \in [R]$ . Lastly, for  $i \in [n]$ , assign  $\hat{X}(i, \cdot)$  to  $\hat{C}_j$  if

$$\arg \max_{s \in \mathcal{S}_n} \langle \hat{X}(i, \cdot), s \rangle = s_j.$$

---

**Algorithm 2** Seeded nearest neighbor subspace clustering

---

Initialize  $\mathcal{S}_0$  to be a random sampling of  $R$  rows of  $\hat{X}$ .

**for all**  $i \in [n]$  **do**

Let  $\tilde{y}, \tilde{z} \in \mathcal{S}_{i-1}$  be such that  $\langle \tilde{y}, \tilde{z} \rangle = \max_{y, z \in \mathcal{S}_{i-1}} \langle y, z \rangle$

**if**  $\max_{x \in \mathcal{S}_{i-1}} \langle \hat{X}(i, \cdot), x \rangle \leq \langle \tilde{y}, \tilde{z} \rangle$  **then**

$\mathcal{S}_i = (\mathcal{S}_{i-1} \setminus \{\tilde{z}\}) \cup \{\hat{X}(i, \cdot)\}$

**end if**

**end for**

Denote  $\mathcal{S}_n = \{s_1, \dots, s_R\}$

Initialize  $R$  clusters  $\hat{C}_1 = \{s_1\}, \dots, \hat{C}_R = \{s_R\}$

**for all**  $i \in [n]$  **do**

Let  $\hat{\tau}(i) = \arg \max_{j \in [R]} \langle \hat{X}(i, \cdot), s_j \rangle$

$\hat{C}_{\hat{\tau}(i)} = \hat{C}_{\hat{\tau}(i)} \cup \{\hat{X}(i, \cdot)\}$

**end for**

---

As encapsulated in the next lemma, this procedure, summarized in Algorithm 2, yields an asymptotically perfect clustering of the rows of  $\hat{X}$  for HSBM’s under mild model assumptions.

**Lemma 6.** *Let  $G \sim \text{HSBM}(n, \bar{\pi}, \{\bar{\pi}_i\}_{i=1}^R, \xi \xi^T)$  satisfying Assumptions 1 and 2, and suppose further that  $\pi_{\min} := \min_i \pi(i) > 0$ . Then asymptotically almost surely,*

$$\min_{\sigma \in \mathcal{S}_R} \sum_i \mathbb{1}\{\hat{\tau}(i) \neq \sigma(\tau(i))\} = 0,$$

where  $\tau : [n] \rightarrow [R]$  is the true assignment of vertices to subgraphs, and  $\hat{\tau}$  is the assignment given by our clustering procedure above.

Under only our “affinity assumption”—namely that  $q > p-k$ -means cannot provide a provably perfect clustering of vertices. This is a consequence of the fact that the number of clusters we seek is far less than the total number of distinct latent positions. As a notional example, consider a graph with two subgraphs, each of which is an SBM with two blocks. The representation of such a graph in terms of its latent positions is illustrated in Figure 1. We are interested in clustering the vertices into subgraphs, i.e., we want to assign the points to their corresponding cones (depicted via the shaded light blue and pink areas). If we denote by  $\pi_1, \pi_2$ , and  $\pi_3$  the fraction of red, green, and blue colored points, respectively, then a  $k$ -means clustering of the colored points into two clusters might, depending on the distance between the points and  $\pi_1, \pi_2, \pi_3$ , yield two clusters with cluster centroids inside the same cone – thereby assigning vertices from different subgraphs to the same cluster. That is to say, if the subgraphs’ sizes in Figure 1 are sufficiently unbalanced, then  $k$ -means clustering could yield a clustering in which the yellow, green, and blue colored points are assigned to one cluster, and the red colored points are assigned to another cluster. In short,  $k$ -means is not a subspace clustering algorithm, and the subspace and

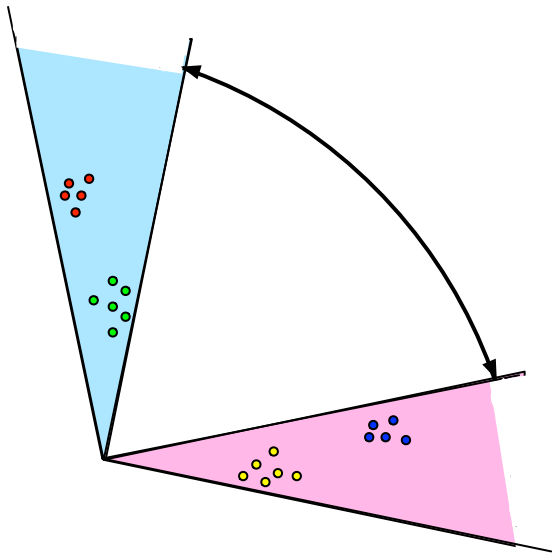


Fig. 1: Subgraphs vs. clustering: Note that if the fraction of points in the pink cone is sufficiently large,  $K$ -means clustering (with  $K = 2$ ) will not cluster the vertices into the canonical subgraphs.

affinity assumptions made in our HSBM formulation (Assumptions 1, 2, 3 and 4) render  $k$ -means suboptimal for uncovering the subgraph structure in our model. Understanding the structure uncovered by  $k$ -means in our HSBM setting, while of interest, is beyond the scope of this manuscript.

Note that  $p$  being small ensures that the subgraphs of interest, namely the  $H_i$ 's, lie in nearly orthogonal subspaces of  $\mathbb{R}^D$ . Our clustering procedure is thus similar in spirit to the subspace clustering procedure of [42].

**Remark 3.** In what follows, we will assume that  $R$ , the number of induced SBM subgraphs in  $G$ , and  $D$  are known a priori. In practice, however, we often need to estimate both  $D$  (prior to embedding) and  $R$  (prior to clustering). To estimate  $D$ , we can use singular value thresholding [43] to estimate  $D$  from a partial SCREE plot. While we can estimate  $R$  via traditional techniques—i.e., measuring the validity of the clustering provided by Algorithm 2 over a range of  $R$  via silhouette width (see [44, Chapter 3])—we propose an alternate estimation procedure tuned to our algorithm. For each  $k = 2, 3, \dots, \widehat{D}$ , we run Algorithm 2 with  $R = k$ , and repeat this procedure  $n_{MC}$  times. For each  $k$ , and each  $i = 1, 2, \dots, n_{MC}$  compute

$$\phi_i^{(k)} = \max_{s, t \in S_n} \langle s, t \rangle,$$

and compute

$$\phi^{(k)} = \frac{1}{n_{MC}} \sum_{i=1}^{n_{MC}} \phi_i^{(k)}.$$

If the true  $R$  is greater than or equal to  $k$ , then we expect  $\phi^{(k)}$  to be small by construction. If  $k$  is bigger

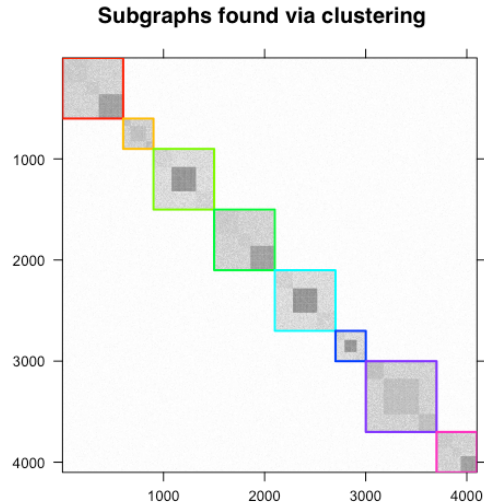


Fig. 2: Depiction of the adjacency matrix of a two-level HSBM graph with 3 distinct motifs. In the above  $4100 \times 4100$  grid, if an edge exists in  $G$  between vertices  $i$  and  $j$ , the corresponding  $i, j$ -th cell in the grid is black. The cell is white if no edge is present. The subgraphs corresponding to motifs are  $H_1, H_4$ , and  $H_8$ ;  $H_2$ , and  $H_7$ ; and  $H_3, H_5$ , and  $H_6$ .

than the true  $R$ , then at least two of the vectors in  $S_n$  would lie in the same subspace; i.e., their dot product would be large. Hence, we would expect the associated  $\phi^{(k)}$  to be large. We employ standard “elbow-finding” methodologies [45] to find the value of  $k$  for which  $\phi^{(k)}$  goes from small to large, and this  $k$  will be our estimate of  $R$ . As Algorithm 2 has running time linear in  $n$ , with a bounded number of Monte Carlo iterates, this estimation procedure also has running time linear in  $n$ .

Post-clustering, a further question of interest is to determine which of those induced subgraphs are structurally similar. We define a motif as a collection of distributionally “equivalent”—in a sense that we will make precise in Definition 7—RDGP graphs. An example of a HSBM graph with 8 blocks in 3 motifs is presented in Figure 2. More precisely, we define a *motif*—namely, an equivalence class of random graphs—as follows.

**Definition 7.** Let  $(A, X) \sim RDPG(F)$  and  $(B, Y) \sim RDPG(G)$ . We say that  $A$  and  $B$  are of the same *motif* if there exists a unitary transformation  $U$  such that  $F = G \circ U$ .

To detect the presence of motifs among the induced subgraphs  $\{\widehat{H}_1, \dots, \widehat{H}_R\}$ , we adopt the nonparametric test procedure of [28] to determine whether two RDGP graphs have the same underlying distribution. The principal result of that work is the following:

**Theorem 8.** Let  $(A, X) \sim RDPG(F)$  and  $(B, Y) \sim RDPG(G)$  be  $d$ -dimensional random dot product graphs.

Consider the hypothesis test

$$H_0: F = G \circ U \quad \text{against} \quad H_A: F \neq G \circ U.$$

Denote by  $\hat{X} = \{\hat{X}_1, \dots, \hat{X}_n\}$  and  $\hat{Y} = \{\hat{Y}_1, \dots, \hat{Y}_m\}$  the adjacency spectral embedding of  $A$  and  $B$ , respectively. Define the test statistic  $T_{n,m} = T_{n,m}(\hat{X}, \hat{Y})$  as follows:

$$T_{n,m}(\hat{X}, \hat{Y}) = \frac{1}{n(n-1)} \sum_{j \neq i} \kappa(\hat{X}_i, \hat{X}_j) - \frac{2}{mn} \sum_{i=1}^n \sum_{k=1}^m \kappa(\hat{X}_i, \hat{Y}_k) + \frac{1}{m(m-1)} \sum_{l \neq k} \kappa(\hat{Y}_k, \hat{Y}_l) \quad (3)$$

where  $\kappa$  is a radial basis kernel, e.g.,  $\kappa = \exp(-\|\cdot - \cdot\|^2/\sigma^2)$ . Suppose that  $m, n \rightarrow \infty$  and  $m/(m+n) \rightarrow \rho \in (0, 1)$ . Then under the null hypothesis of  $F = G \circ U$ ,

$$|T_{n,m}(\hat{X}, \hat{Y}) - T_{n,m}(X, YW)| \xrightarrow{\text{a.s.}} 0 \quad (4)$$

and  $|T_{n,m}(X, YW)| \rightarrow 0$  as  $n, m \rightarrow \infty$ , where  $W$  is any orthogonal matrix such that  $F = G \circ W$ . In addition, under the alternative hypothesis of  $F \neq G \circ U$ , there exists an orthogonal matrix  $W \in \mathbb{R}^{d \times d}$ , depending on  $F$  and  $G$  but independent of  $m$  and  $n$ , such that

$$|T_{n,m}(\hat{X}, \hat{Y}) - T_{n,m}(X, YW)| \xrightarrow{\text{a.s.}} 0, \quad (5)$$

and  $|T_{n,m}(X, YW)| \rightarrow c > 0$  as  $n, m \rightarrow \infty$ .

Theorem 8 allows us to formulate the problem of detecting when two graphs  $A$  and  $B$  belong to the same motif as a hypothesis test. Furthermore, under appropriate conditions on  $\kappa$  (conditions satisfied when  $\kappa$  is a Gaussian kernel with bandwidth  $\sigma^2$  for fixed  $\sigma$ ), the hypothesis test is consistent for any two arbitrary but fixed distributions  $F$  and  $G$ , i.e.,  $T_{n,m}(X, Y) \rightarrow 0$  as  $n, m \rightarrow \infty$  if and only if  $F = G$ . We are presently working to extend results on the consistency of adjacency spectral embedding and two-sample hypothesis testing (i.e., Theorem 8 and [29]) from the current setting of random dot product graphs to more general random graph models, with particular attention to scale-free and small-world graphs. However, the extension of these techniques to more general random graphs is beset by intrinsic difficulties. For example, even extending motif detection to general latent position random graphs is confounded by the non-identifiability inherent to graphon estimation. Complicating matters further, there are few random graph models that are known to admit parsimonious sufficient statistics suitable for subsequent classical estimation procedures.

### 3 DETECTING HIERARCHICAL STRUCTURE IN THE HSBM

Combining the above inference procedures, our algorithm, as depicted in Algorithm 1, proceeds as follows. We first cluster the adjacency spectral embedding of the graph  $G$  to obtain the first-order, large-scale block memberships. We then employ the nonparametric test

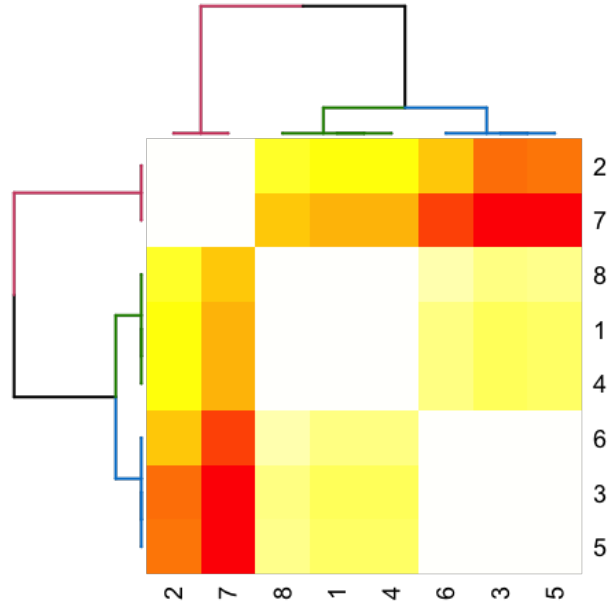


Fig. 3: Heatmap depicting the dissimilarity matrix  $\hat{S}$  produced by Algorithm 1 for the 2-level HSBM depicted in Figure 2. We apply hierarchical clustering to  $\hat{S}$  (with the resulting dendrogram clustering displayed) demonstrating the which recover the three distinct motifs.

procedure outlined in [28] to determine similar induced subgraphs (motifs) associated with these blocks. We iterate this process to obtain increasingly refined estimates of the overall graph structure. In Step 6 of Algorithm 1, we recurse on a representative subgraph (e.g., the largest subgraph) within each motif; embedding the subgraph into  $\mathbb{R}^d$  (not  $\mathbb{R}^D$ ) as Step 1 of Algorithm 1. Ideally, we would leverage the full collection of subgraphs from each motif in this recursion step. However, the subgraphs within a motif may be of differing orders and meaningfully averaging or aligning them (see [46]) requires novel regularization which, though interesting, is beyond the scope of the present manuscript.

Before presenting our main theorem in the 2-level setting, Theorem 9, we illustrate the steps of our method in the analysis of the 2-level synthetic HSBM graph depicted in Figure 2. The graph has 4100 vertices belonging to 8 different blocks of size  $\vec{n} = (300, 600, 600, 600, 700, 600, 300, 400)$  with three distinct motifs. The block probability matrices corresponding to these motifs are given by

$$B_1 = \begin{bmatrix} 0.3 & 0.25 & 0.25 \\ 0.25 & 0.3 & 0.25 \\ 0.25 & 0.25 & 0.7 \end{bmatrix}; \quad B_2 = \begin{bmatrix} 0.4 & 0.25 & 0.25 \\ 0.25 & 0.4 & 0.25 \\ 0.25 & 0.25 & 0.4 \end{bmatrix};$$

$$B_3 = \begin{bmatrix} 0.25 & 0.2 & 0.2 \\ 0.2 & 0.8 & 0.2 \\ 0.2 & 0.2 & 0.25 \end{bmatrix},$$

and the inter-block edge probability is bounded by  $p = 0.01$ .

The algorithm does indeed detect three motifs, as depicted in Figure 3. The figure presents a heat map depiction of  $\widehat{S}$ , and the similarity of the communities is represented on the spectrum between white and red, with white representing highly similar communities and red representing highly dissimilar communities. From the figure, we correctly see there are three distinct motif communities,  $\{\widehat{H}_3, \widehat{H}_7\}$ ,  $\{\widehat{H}_1, \widehat{H}_2, \widehat{H}_8\}$ , and  $\{\widehat{H}_4, \widehat{H}_5, \widehat{H}_6\}$ , corresponding to stochastic blockmodels with the following block probability matrices

$$\widehat{B}_1 = \begin{bmatrix} 0.27 & 0.25 \\ 0.25 & 0.72 \end{bmatrix}; \quad \widehat{B}_2 = \begin{bmatrix} 0.41 & 0.27 & 0.26 \\ 0.27 & 0.40 & 0.25 \\ 0.26 & 0.25 & 0.41 \end{bmatrix}.$$

$$\widehat{B}_3 = \begin{bmatrix} 0.22 & 0.20 \\ 0.20 & 0.80 \end{bmatrix}.$$

We note that even though the vertices in the HSBM are perfectly clustered into the subgraphs (i.e., for  $i \in [8]$ ,  $\widehat{H}_i = H_i$  for all  $i$ ), the actual  $B$ 's differ slightly from their estimates, but this difference is quite small.

The performance of Algorithm 1 in this simulation setting can be seen as a consequence of Theorem 9 below, in which we prove that under modest assumptions on an underlying 2-level hierarchical stochastic block model, Algorithm 2 yields a consistent estimate of the dissimilarity matrix  $S := [T_{n_i, n_j}(H_i, H_j)]$ .

**Theorem 9.** *Suppose  $G$  is a hierarchical stochastic blockmodel satisfying Assumptions 1 and 2. Suppose that  $R$  is fixed and the  $\{H_r\}$  correspond to  $M$  different motifs, i.e., the set  $\{\xi_1, \xi_2, \dots, \xi_R\}$  has  $M \leq R$  distinct elements. Given the assumptions of Theorem 5 and Lemma 6, the procedure in Algorithm 1 yields perfect estimates  $\widehat{H}_1 = H_1, \dots, \widehat{H}_R = H_R$  of  $H_1, \dots, H_R$  and  $\widehat{S}$  of  $S$  asymptotically almost surely.*

*Proof:* By Lemma 6, the clustering provided by Step 2 of Algorithm 1 will be perfect asymptotically almost surely. Given this,  $\widehat{H}_1 = H_1, \dots, \widehat{H}_R = H_R$  are consistent estimates of  $H_1, \dots, H_R$ . Theorem 8 then implies that  $\widehat{S}$  yields a consistent estimate of  $S$ ; i.e.; for each  $i, j$ ,  $|\widehat{S}(i, j) - S(i, j)| \rightarrow 0$  as  $n \rightarrow \infty$ .  $\square$

With assumptions as in Theorem 9, any level  $\gamma$  test using  $S_{ij}$  corresponds to an at most level  $\gamma + 2\eta$  test using  $\widehat{S}_{ij}$ . In this case, asymptotically almost surely, the  $p$ -values of entries of  $\widehat{S}$  corresponding to different motifs will all converge to 0 as  $n\pi_{\min} \rightarrow \infty$ , and the  $p$ -values of entries of  $\widehat{S}$  corresponding to the same motifs will all be bounded away from 0 as  $n\pi_{\min} \rightarrow \infty$ . This immediately leads to the following corollary.

**Corollary 10.** *With assumptions as in Theorem 9, clustering the matrix of  $p$ -values associated with  $\widehat{S}$  yields a consistent clustering of  $\{\widehat{H}_i\}_{i=1}^R$  into motifs.*

Theorem 9 provides a proof of concept inference result for our algorithm for graphs with simple hierarchical structure, and we will next extend our setting and theory to a more complex hierarchical setting.

## 4 MULTILEVEL HSBM

In many real data applications (see for example, Section 5), the hierarchical structure of the graph extends beyond two levels. We now extend the HSBM model of Definition 3—which, for ease of exposition, was initially presented in the 2-level hierarchical setting—to incorporate more general hierarchical structure. With the HSBM of Definition 3 being a 2-level HSBM (or 2-*HSBM*), we inductively define an  $\ell$ -level HSBM (or  $\ell$ -*HSBM*) for  $\ell \in \mathbb{Z} \geq 3$  as follows.

**Definition 11** ( $\ell$ -level Hierarchical stochastic blockmodel  $\ell$ -*HSBM*). We say that  $(X, A) \sim \text{RDPG}(F^{(\ell)})$  is an instantiation of a  $D^{(\ell)}$ -dimensional  $\ell$ -level HSBM if the distribution  $F^{(\ell)}$  can be written as

$$F^{(\ell)} = \sum_{i=1}^{R^{(\ell)}} \pi^{(\ell)}(i) F_i^{(\ell)}, \quad (6)$$

where

- i.  $\bar{\pi}^{(\ell)} \in (0, 1)^{R^{(\ell)}}$  with  $\sum_i \pi^{(\ell)}(i) = 1$ ;
- ii.  $F^{(\ell)}$  has support on the rows of  $[\xi_1^{(\ell)} | \xi_2^{(\ell)} | \dots | \xi_{R^{(\ell)}}^{(\ell)}]^T$ , where for each  $i \in [R^{(\ell)}]$ ,  $F_i^{(\ell)}$  has support on the rows of  $(\xi_i^{(\ell)})^T$ .
- iii. For each  $i \in [R^{(\ell)}]$ , an RDPG graph drawn according to  $(Y, B) \sim \text{RDPG}(F_i^{(\ell)})$  is an  $h$ -level HSBM with  $h \leq \ell - 1$  with at least one such  $h = \ell - 1$ .

Simply stated, an  $\ell$ -level HSBM graph is an RDPG (in fact, it is an SBM with potentially many more than  $R^{(\ell)}$  blocks) for which the vertex set can be partitioned into  $R^{(\ell)}$  subgraphs—where  $(\xi_i^{(\ell)})^T \in \mathbb{R}^{K_i^{(\ell)} \times D^{(\ell)}}$  denotes the matrix whose rows are the latent positions characterizing the block probability matrix for subgraph  $i$ —each of which is itself an  $h$ -level HSBM with  $h \leq \ell - 1$  with at least one such  $h = \ell - 1$ .

As in the 2-level case, to ease notation and facilitate theoretical developments, in this paper we will make the following assumptions on the more general  $\ell$ -level HSBM. Letting  $(X, A) \sim \text{RDPG}(F^{(\ell)})$  be an instantiation of a  $D^{(\ell)}$ -dimensional  $\ell$ -level HSBM, we further assume: **Assumption 3:** (Multilevel affinity) For each  $k \in \{2, 3, \dots, \ell\}$  the constants

$$q^{(k)} := \min_{i,j,h} \langle \xi_i^{(k)}(:, j), \xi_i^{(k)}(:, h) \rangle, \quad (7)$$

$$p^{(k)} := \max_{i \neq j} \max_{m,h} \langle \xi_i^{(k)}(:, h), \xi_j^{(k)}(:, m) \rangle \quad (8)$$

satisfy  $p^{(k)} < q^{(k)}$ .

**Assumption 4:** (Subspace structure) For each  $i \in [R^{(\ell)}]$ ,



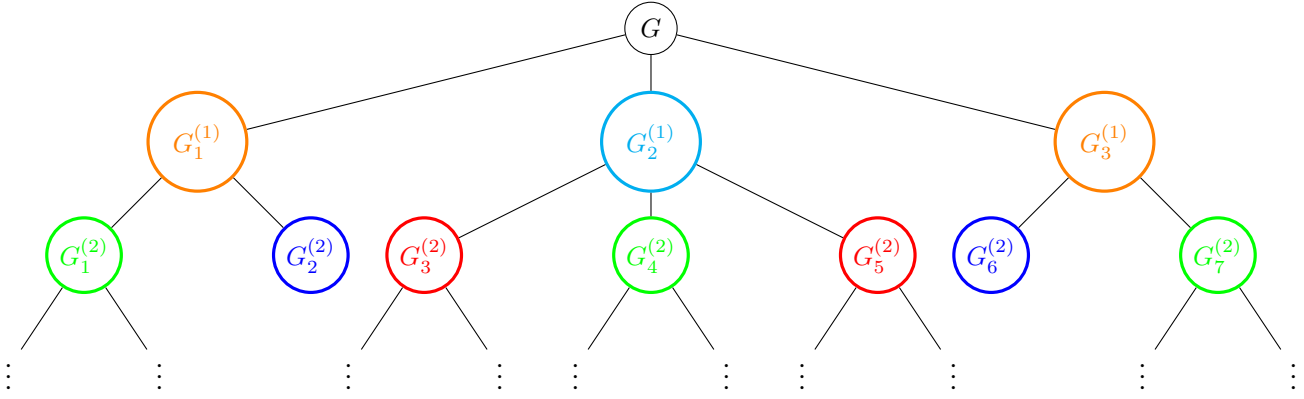


Fig. 4: Notional depiction of a general hierarchical graph structure. The colored nodes in the first and second level of the tree (below the root node) correspond to induced subgraphs and associated motifs.

$F_i^{(\ell)}$  has support on the rows of  $(\xi_i^{(\ell)})^T$ , which collectively satisfy

$$\begin{bmatrix} (\xi_1^{(\ell)})^T \\ (\xi_2^{(\ell)})^T \\ \vdots \\ (\xi_{R^{(\ell)}}^{(\ell)})^T \end{bmatrix} = \underbrace{\begin{bmatrix} (\xi_1^{(\ell-1)})^T & 0 & \cdots & 0 \\ 0 & (\xi_2^{(\ell-1)})^T & \cdots & 0 \\ \vdots & \vdots & \ddots & \vdots \\ 0 & 0 & \cdots & (\xi_{R^{(\ell-1)}}^{(\ell-1)})^T \end{bmatrix}}_{Z^{(\ell)}} + \mathcal{A}^{(\ell)}, \quad (9)$$

where  $Z^{(\ell)} \circ \mathcal{A}^{(\ell)} = 0$  ( $\circ$  again being the Hadamard product). For each  $i \in [R^{(\ell)}]$ , an RDPG graph drawn according to  $(Y, B) \sim \text{RDPG}(F_i^{(\ell-1)})$  where  $F_i^{(\ell-1)}$  has support on the rows of  $(\xi_i^{(\ell-1)} \in \mathbb{R}^{K_i^{(\ell-1)} \times D_i^{(\ell-1)}})^T$  and is an at most  $\ell - 1$ -level HSBM (with at least one subgraph being an  $(\ell - 1)$ -level HSBM). In addition, we assume similar subspace structure recursively at every level of the hierarchy.

**Remark 4.** As was the case with Assumption 2, Assumption 4 plays a crucial role in our algorithmic development. Indeed, under this assumption we can view successive levels of the hierarchical HSBM as RDPG's in successively smaller dimensions. Indeed, it is these  $(Y, B) \sim \text{RDPG}(F_i^{(\ell-1)})$  which we embed in Step 3 of Algorithm 1, and we embed them into the smaller  $\mathbb{R}^{D_i^{\ell-1}}$  rather than  $\mathbb{R}^{D^{(\ell)}}$ . For example, suppose  $G$  is an  $\ell$ -level HSBM, and  $G$  has  $R$  subgraphs each of which is an  $(\ell - 1)$ -level HSBM. Furthermore suppose that each of these subgraphs itself has  $R$  subgraphs each of which is an  $(\ell - 2)$ -level HSBM, and so on. If the SBM's at the lowest level are all  $d$ -dimensional, then  $G$  can be viewed as an  $R^{\ell-1}d$ -dimensional RDPG. In practice, to avoid this curse of dimensionality, we could embed each subgraph at level  $k \leq \ell$  into  $R$  dimensions and still practically uncover the subgraph (but not the motif!) structure. This assumption also reinforces the affinity structure of the subgraphs, which is a key component of our theoretical developments.

In the 2-level HSBM setting, we can provide theoret-

ical results on the consistency of our motif detection procedure, Algorithm 1. As it happens, in this simpler setting, the algorithm terminates after Step 6; that is, after clustering the induced subgraphs into motifs. There is no further recursion on these motifs. We next extend Theorem 9 to the multi-level HSBM setting as follows. In the following theorem, for an RDPG  $G = (X, A)$ , let  $\hat{X}_G$  be the ASE of  $G$  and let  $X_G = X$  be the true latent positions of  $G$ ; i.e.,  $\mathbb{E}(A) = XX^\top$ .

**Theorem 12.** *With notation as above, let  $(X, A) \sim \text{RDPG}(F^{(\ell)})$  be an instantiation of a  $D^{(\ell)}$ -dimensional,  $\ell$ -level HSBM with  $\ell$  fixed. Given Assumptions 3 and 4, further suppose that for each  $k \in \{2, 3, \dots, \ell\}$  every  $k$ -level HSBM subgraph,  $G$ , of  $(X, A)$  satisfies*

- i. *the number of components in the mixture, Eq. 6 for  $G$ , which we shall denote by  $R^G$ , is known and fixed with respect to  $n$ , and  $\{H_r^G\}_{r=1}^{R^G}$  are these  $R^G$  subgraphs of  $G$ ; additionally, the  $R^G$  mixture coefficients  $\pi_G(\cdot)$  (associated with Eq. 6 for  $G$ ) are all strictly greater than 0;*
- ii. *if  $G$  is  $D^G$  dimensional, then these  $R^G$  subgraphs—when viewed as the subgraphs corresponding the diagonal blocks of  $Z^G$  of Eq. 9 to be embedded into  $< D^G$  dimensions as in Remark 4—correspond to  $M^G$  different motifs with  $M^G$  fixed with respect to  $n$ .*

*It follows then that for all such  $G$ , the procedure in Algorithm 1 simultaneously yields perfect estimates  $\hat{H}_1^G = H_1^G$ ,  $\hat{H}_2^G = H_2^G, \dots, \hat{H}_{R^G}^G = H_{R^G}^G$  of  $\{H_r^G\}_{r=1}^{R^G}$  asymptotically almost surely. It follows then that for for each such  $G$ ,  $\hat{S}^G = [T(\hat{X}_{\hat{H}_i^G}, \hat{X}_{\hat{H}_j^G})]$  yield consistent estimates of  $S^G = [T(X_{H_i^G}, X_{H_j^G})]$ , which allows for the asymptotically almost surely perfect detection of the  $M^G$  motifs.*

We note here that in Theorem 12,  $\ell$  and the total number of subgraphs at each level of the hierarchy are fixed with respect to  $n$ . As  $n$  increases, the size of each subgraph at each level is also increasing (linearly in  $n$ ), and therefore any separation between  $p^{(k)}$  and  $q^{(k)}$  at level  $k$  will be sufficient to perfectly separate the subgraphs asymptoti-

cally almost surely. The proof of the above theorem then follows immediately from Theorem 9 and induction on  $\ell$ , and so is omitted.

Theorem 12 states that, under modest assumptions, Algorithm 1 yields perfect motif detection and classification at every level in the hierarchy. From a technical viewpoint, this theorem relies on a  $2 \rightarrow \infty$  norm bound on the residuals of  $\hat{X}$  about  $X$  (see 15), which is crucial to the perfect recovery of precisely the  $R_G$  large-scale subgraphs. This bound, in turn, only guarantees this perfect recovery of when the average degree is at least of order  $\sqrt{n} \log^2(n)$ . We surmise that for subsequent inference tasks that are more robust to the identification of the large-scale subgraphs, results can be established in sparser regimes.

Moreover, when applying this procedure to graphs which violate our HSBM model assumptions (for example, when applying the procedure to real data), we encounter error propagation inherent to recursive procedures. In Algorithm 1, there are three main sources of error propagation: errorful clusterings; the effect of these errorfully-inferred subgraphs on  $\hat{S}$ ; and subsequent clustering and analysis within these errorful subgraphs. We briefly address these three error sources below.

First, finite-sample clustering is inherently errorful and misclustered vertices contribute to degradation of power in the motif detection test statistic. While we prove the asymptotic consistency of our clustering procedure in Lemma 6, there are a plethora of other graph clustering procedures we might employ in the small-sample setting, including modularity-based methods such as Louvain [8] and *fastgreedy* [47], and random walk-based methods such as *walktrap* [10]. Understanding the impact that the particular clustering procedure has on subsequent motif detection is crucial, as is characterizing the common properties of misclustered vertices; e.g., in a stochastic block model, are misclustered vertices overwhelmingly likely to be low-degree?

Second, although testing based on  $T$  is asymptotically robust to a modest number of misclustered vertices, namely  $o(\max_i n\pi(i))$  vertices, the finite-sample robustness of this test statistic remains open. Lastly, we need to understand the robustness properties of further clustering these errorfully observed motifs. In [48], the authors propose a model for errorfully observed random graphs, and study the subsequent impact of the graph error on vertex classification. Adapting their model and methodology to the framework of spectral clustering will be essential for understanding the robustness properties of our algorithm, and is the subject of present research.

## 5 EXPERIMENTS

We next apply our algorithm to two real data networks: the *Drosophila* connectome from [6] and the Friendster

social network.

### 5.1 Motif detection in the *Drosophila* Connectome

The *cortical column conjecture* suggests that neurons are connected in a graph which exhibits motifs representing repeated processing modules. (Note that we understand that there is controversy surrounding the definition and even the existence of ‘‘cortical columns’’; our consideration includes ‘‘generic’’ recurring circuit motifs, and is not limited to the canonical Mountcastle-style column [4].) While the full cortical connectome necessary to rigorously test this conjecture is not yet available even on the scale of fly brains, in [6] the authors were able to construct a portion of the *Drosophila* fly medulla connectome which exhibits columnar structure.

This graph is constructed by first constructing the full connectome between 379 named neurons (believed to be a single column) and then sparsely reconstructing the connectome between and within surrounding columns via a semi-automated procedure. The resulting connectome<sup>2</sup> has 1748 vertices in its largest connected component, the adjacency matrix of which is visualized in the upper left of Figure 5. We visualize our Algorithm 1 run on this graph in Figure 5. First we embed the graph into  $\mathbb{R}^{13}$  (13 chosen according to the singular value thresholding method applied to a partial SCREE plot; see Remark 3) and, to alleviate sparsity concerns, project the embedding onto the sphere. The resulting points are then clustered into  $\hat{R} = 8$  clusters ( $\hat{R}$  chosen as in Remark 3) of sizes  $|V(\hat{H}_1)| = 176$ ,  $|V(\hat{H}_2)| = 237$ ,  $|V(\hat{H}_3)| = 434$ ,  $|V(\hat{H}_4)| = 237$ ,  $|V(\hat{H}_5)| = 142$ ,  $|V(\hat{H}_6)| = 237$ ,  $|V(\hat{H}_7)| = 115$ , and  $|V(\hat{H}_8)| = 170$  vertices. These clusters are displayed in the upper right of Figure 5. We then compute the corresponding  $\hat{S}$  matrix after re-embedding each of these clusters (bottom of Figure 5). In the heat map representation of  $\hat{S}$ , the similarity of the communities is represented on the spectrum between white and red, with white representing highly similar communities and red representing highly dissimilar communities. For example, the bootstrapped  $p$ -value (from 200 bootstrap samples) associated with  $T(\hat{H}_6, \hat{H}_8)$  is 0.195, with  $T(\hat{H}_2, \hat{H}_6)$  is 0.02 and with  $T(\hat{H}_6, \hat{H}_1)$  is 0.005.

We next apply hierarchical clustering to  $\hat{S}$  to uncover the repeated motif structure (with the resulting dendrogram displayed in Figure 5). Both methods uncovered two repeated motifs, the first consisting of subgraphs 1 and 4 and the second consisting of subgraphs 2, 6, and 8. Note that the hierarchical clustering also reveals 2nd level motif repetition within the second motif given by  $\{6, 8\}$ . Indeed, our method uncovers repeated *hierarchical* structure in this connectome, and we are presently

<sup>2</sup> available from the open connectome project <http://openconnectome.org/graph-services/download/> (see *fly*)

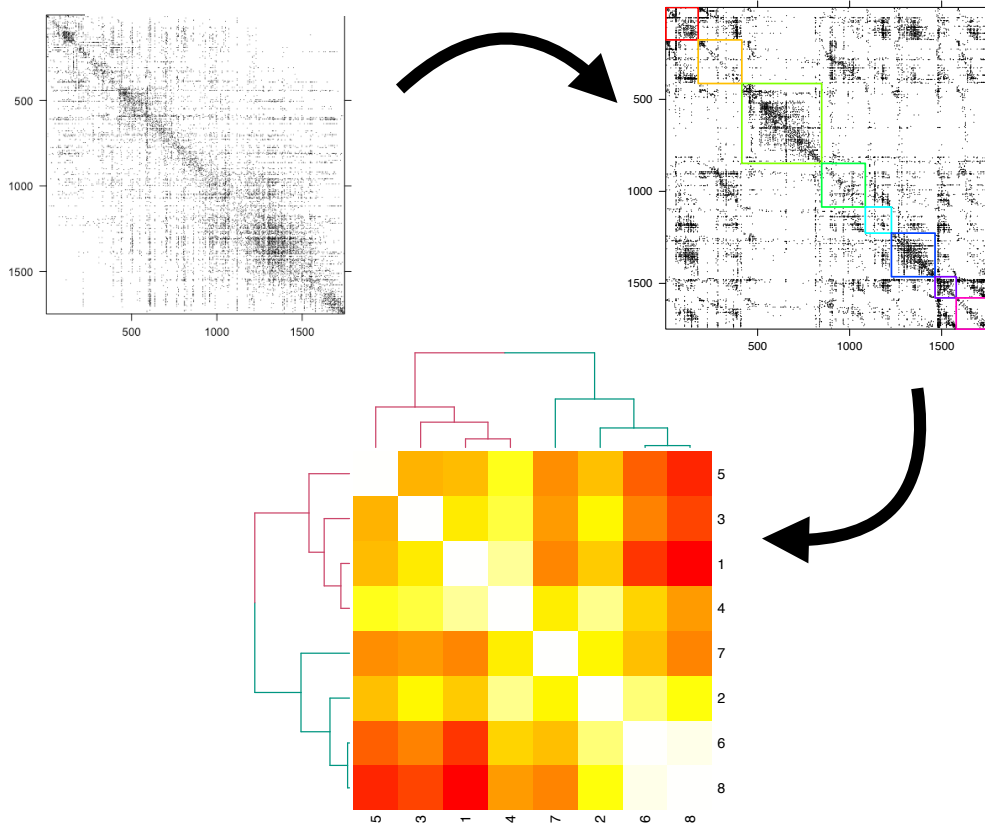


Fig. 5: Visualization of our method applied to the *Drosophila* connectome. We show the adjacency matrix (upper left), the clustering derived via ASE, projection to the sphere and clustering via Algorithm 2, and lastly  $\hat{S}$  calculated from these clusters. Clustering the subgraphs based on this  $\hat{S}$  suggests two repeated motifs:  $\{1, 4\}$  and  $\{2, 6, 8\}$ . Note that the hierarchical clustering also reveals 2nd level motif repetition within the second motif given by  $\{6, 8\}$ .

working with neurobiologists to determine the biological significance of our clusters and motifs.

## 5.2 Motif detection in the Friendster network

We next apply our methodology to analyze and classify communities in the Friendster social network. The Friendster social network contains roughly 60 million users and 2 billion connections/edges. In addition, there are roughly 1 million communities at the local scale. Because we expect the social interactions in these communities to inform the function of the different communities, we expect to observe distributional repetition among the graphs associated with these communities.

Implementing Algorithm 1 on the very large Friendster graph presents computational challenges. To overcome this challenge in scalability, we use the specialized SSD-based graph processing engine `FlashGraph` [49], which is designed to analyze graphs with billions of nodes. With `FlashGraph`, we adjacency spectral embed the Friendster adjacency matrix into  $\mathbb{R}^{14}$ —where  $\hat{D} = 14$  is chosen using singular value thresholding on the partial SCREE plot (see Remark 3). Using the model selection

methodology outlined in Remark 3, we find the best coarse-grained clustering of the graph is achieved with  $\hat{R} = 15$  large-scale clusters ranging in size from  $10^6$  to 15.6 million vertices (note that to alleviate sparsity concerns, we projected the embedding onto the sphere before clustering). After re-embedding the induced subgraphs associated with these 15 clusters, we use a linear time estimate of the test statistic  $T$  to compute  $\hat{S}$ , the matrix of estimated pairwise dissimilarities among the subgraphs. See Figure 6 for a heat map depicting  $\hat{S} \in \mathbb{R}^{15 \times 15}$ . In the heat map, the similarity of the communities is represented on the spectrum between white and red, with white representing highly similar communities and red representing highly dissimilar communities. From the figure, we can see clear repetition in the subgraph distributions; for example, we see a repeated motif including subgraphs  $\{\hat{H}_5, \hat{H}_4, \hat{H}_3, \hat{H}_2\}$  and a clear motif including subgraphs  $\{\hat{H}_{10}, \hat{H}_{12}, \hat{H}_9\}$ .

Formalizing the motif detection step, we next employ hierarchical clustering to cluster  $\hat{S}$  into motifs; see Figure 6 for the corresponding hierarchical clustering dendrogram, which suggests that our algorithm does in fact uncover repeated motif structure at the coarse-grained

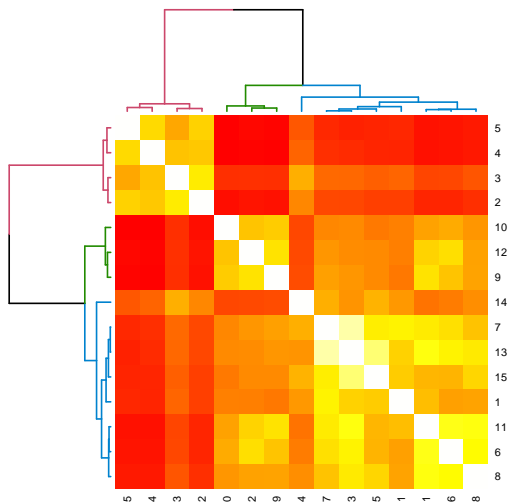


Fig. 6: Heat map depiction of the level one Friendster estimated dissimilarity matrix  $\hat{S} \in \mathbb{R}^{15 \times 15}$ . In the heat map, the similarity of the communities is represented on the spectrum between white and red, with white representing highly similar communities and red representing highly dissimilar communities. In addition, we cluster  $\hat{S}$  using hierarchical clustering and display the associated hierarchical clustering dendrogram.

level in the Friendster graph. While it may be difficult to draw meaningful inference from repeated motifs at the scale of hundreds of thousands to millions of vertices, if these motifs are capturing a common HSBM structure within the subgraphs in the motif, then we can employ our algorithm recursively on each motif to tease out further hierarchical structure.

Exploring this further, we consider three subgraphs  $\{\hat{H}_2, \hat{H}_8, \hat{H}_{15}\}$ , two of which are in the same motif (8 and 15) and both differing significantly from subgraph 2 according to  $\hat{S}$ . We embed these subgraphs into  $\mathbb{R}^{26}$  (26 chosen as outlined in Remark 3), perform a Procrustes alignment of the vertex sets of the three subgraphs, cluster each into 4 clusters (4 chosen to optimize silhouette width in  $k$ -means clustering), and estimate both the block connection probability matrices,

$$\hat{P}_2 = \begin{bmatrix} 0.000045 & 0.00080 & 0.00056 & 0.00047 \\ 0.00080 & 0.025 & 0.0096 & 0.0072 \\ 0.00057 & 0.0096 & 0.012 & 0.0067 \\ 0.00047 & 0.0072 & 0.0067 & 0.023 \end{bmatrix},$$

$$\hat{P}_8 = \begin{bmatrix} 0.0000022 & 0.000031 & 0.000071 & 0.000087 \\ 0.000031 & 0.0097 & 0.00046 & 0.00020 \\ 0.000071 & 0.00046 & 0.0072 & 0.0030 \\ 0.000087 & 0.00020 & 0.003 & 0.016 \end{bmatrix},$$

$$\hat{P}_{15} = \begin{bmatrix} 0.0000055 & 0.00011 & 0.000081 & 0.000074 \\ 0.00011 & 0.014 & 0.0016 & 0.00031 \\ 0.000081 & 0.0016 & 0.0065 & 0.0022 \\ 0.000074 & 0.00031 & 0.0022 & 0.019 \end{bmatrix},$$

and the block membership probabilities  $\hat{\pi}_2, \hat{\pi}_8, \hat{\pi}_{15}$ , for each of the three graphs. We calculate

$$\begin{aligned} \|\hat{P}_2 - \hat{P}_8\|_F &= 0.033; \\ \|\hat{P}_2 - \hat{P}_{15}\|_F &= 0.027; \\ \|\hat{P}_8 - \hat{P}_{15}\|_F &= 0.0058; \\ \|\hat{\pi}_2 - \hat{\pi}_8\| &= 0.043; \\ \|\hat{\pi}_2 - \hat{\pi}_{15}\| &= 0.043; \\ \|\hat{\pi}_8 - \hat{\pi}_{15}\| &= 0.0010; \end{aligned}$$

which suggests that the repeated structure our algorithm uncovers is *SBM substructure*, thus ensuring that we can proceed to apply our algorithm recursively to the subsequent motifs.

As a final point, we recursively apply Algorithm 1 to the subgraph  $\hat{H}_{11}$ . We first embed the graph into  $\mathbb{R}^{26}$  (again, with 26 chosen as outlined in Remark 3). Next, using the model selection methodology outlined in Remark 3, we cluster the vertices into  $\hat{R} = 13$  large-scale clusters of sizes ranging from 500K to 2.7M vertices. We then use a linear time estimate of the test statistic  $T$  to compute  $\hat{S}$  (see Figure 7), and note that there appear to be clear repeated motifs (for example, subgraphs 8 and 12) among the  $\hat{H}$ 's. We run hierarchical clustering to cluster the 13 subgraphs, and note that the associated dendrogram—as shown in Figure 7—shows that our algorithm again uncovered some repeated level-2 structure in the Friendster network. We can, of course, recursively apply our algorithm still further to tease out the motif structure at increasingly fine-grained scale.

Ideally, when recursively running Algorithm 1, we would like to simultaneously embed and cluster all subgraphs in the motif. In addition to potentially reducing embedding variance, being able to efficiently simultaneously embed all the subgraphs in a motif could greatly increase algorithmic scalability in large networks with a very large number of communities at local-scale. In order to do this, we need to understand the nature of the repeated structure within the motifs. This repeated structure can inform an estimation of a motif average (an averaging of the subgraphs within the motif), which can then be embedded into an appropriate Euclidean space in lieu of embedding all of the subgraphs in the motif separately. However, this averaging presents several novel challenges, as these subgraphs may be of very different orders and may be errorfully obtained, which could lead to compounded errors in the averaging step. We are presently working to determine a robust averaging procedure (or a simultaneous embedding procedure akin to JOFC [50]) which exploits the common structure within the motifs.

## 6 CONCLUSION

In summary, we provide an algorithm for community detection and classification for hierarchical stochastic

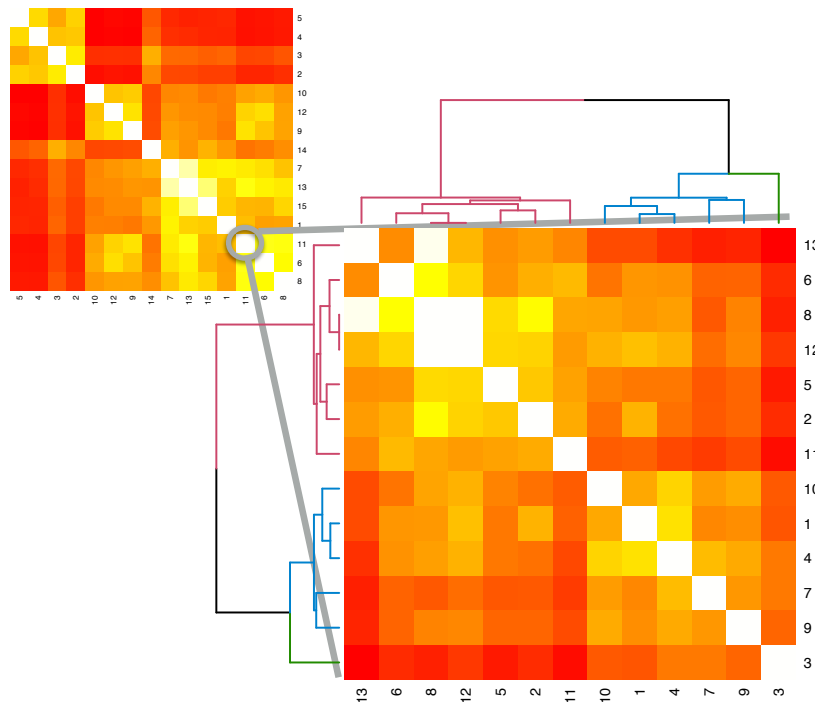


Fig. 7: Heat map depiction of the level two Friendster estimated dissimilarity matrix  $\hat{S} \in \mathbb{R}^{13 \times 13}$  of  $\hat{H}_{11}$ . In the heat map, the similarity of the communities is represented on the spectrum between white and red, with white representing highly similar communities and red representing highly dissimilar communities. In addition, we cluster  $\hat{S}$  using hierarchical clustering and display the associated hierarchical clustering dendrogram.

blockmodels. Our algorithm depends on a consistent lower-dimensional embedding of the graph, followed by a valid and asymptotically powerful nonparametric test procedure for the determination of distributionally equivalent subgraphs known as motifs. In the case of a two-level hierarchical stochastic block model, we establish theoretical guarantees on the consistency of our estimates for the induced subgraphs and the validity of our subsequent tests.

While the hierarchical stochastic block model is a very particular random graph model, the hierarchical nature of the HSBM—that of smaller subgraphs that are densely connected within and somewhat loosely connected across—is a central feature of many networks. Because our results are situated primarily in the context of random dot product graphs, and because random dot product graphs can be used to closely approximate many independent edge graphs [51], we believe that our algorithm can be successfully adapted for the determination of multiscale structure in significantly more intricate models.

By performing community detection and classification on the *Drosophila* connectome and on the social network Friendster, we demonstrate that our algorithm can be feasibly deployed on real (and, in the case of Friendster, large!) graphs. We leverage state-of-the-art software

packages `FlashGraph` and `igraph` to substantially reduce computation time. In both graphs, our algorithm detects and classifies multiple similar communities. Of considerable interest and ongoing research is the analysis of the functional or structural features of these distinct communities. Because our algorithm can be applied recursively to uncover finer-grained structure, we are hopeful that these methods can contribute to a deeper understanding of the implications of statistical subgraph similarity on the structure and function of social and biological networks.

## 7 ACKNOWLEDGMENTS

The authors thank Zheng Da, Disa Mhembere, and Randal Burns for assistance in processing the Friendster graph using `FlashGraph` [49], Gabor Csardi and Edo Airoldi for assistance in implementing our algorithm in `igraph` [52], Daniel L. Sussman for helpful discussions in formulating the HSBM framework, and R. Jacob Vogelstein and Joshua T. Vogelstein for suggesting this line of research. This work is partially supported by the XDATA & GRAPHS programs of the Defense Advanced Research Projects Agency (DARPA).

## REFERENCES

- [1] S. Wasserman and K. Faust, *Social Network Analysis: Methods and Applications*. Cambridge University Press, 1994.
- [2] E. Bullmore and O. Sporns, "Complex brain networks: Graph theoretical analysis of structural and functional systems," *Nature Rev. Neurosci.*, vol. 10, pp. 186–198, 2009.
- [3] D. J. de Solla Price, "Networks of scientific papers," *Science*, vol. 149, pp. 510–515, 1965.
- [4] V. B. Mountcastle, "The columnar organization of the neocortex." *Brain*, vol. 120, no. 4, pp. 701–722, 1997.
- [5] G. Marcus, A. Marblestone, and T. Dean, "The atoms of neural computation," *Science*, vol. 346, no. 6209, pp. 551–552, 2014.
- [6] S. Takemura, A. Bharioke, Z. Lu, A. Nern, S. Vitaladevuni, P. K. Rivlin, W. T. Katz, D. J. Olbris, S. M. Plaza, P. Winston, T. Zhao, J. A. Horne, R. D. Fetter, S. Takemura, K. Blazek, L.-A. Chang, O. Ogundeyi, M. A. Saunders, V. Shapiro, C. Sigmund, G. M. Rubin, L. K. Scheffer, I. A. Meinertzhagen, and D. B. Chklovskii, "A visual motion detection circuit suggested by drosophila connectomics," *Nature*, vol. 500, no. 7461, pp. 175–181, 2013.
- [7] P. J. Bickel and A. Chen, "A nonparametric view of network models and Newman-Girvan and other modularities." *Proceedings of the National Academy of Sciences of the United States of America*, vol. 106, pp. 21 068–73, 2009.
- [8] V. D. Blondel, J.-L. Guillaume, R. Lambiotte, and E. Lefebvre, "Fast unfolding of communities in large networks," *Journal of Statistical Mechanics: Theory and Experiment*, 2008.
- [9] M. Newman and M. Girvan, "Finding and evaluating community structure in networks," *Physical Review*, vol. 69, pp. 1–15, Feb. 2004.
- [10] P. Pons and M. Latapy, "Computing communities in large networks using random walks," in *Proceedings of the 20th international conference on Computer and Information Sciences*, 2005, pp. 284–293.
- [11] M. Rosvall and C. T. Bergstrom, "Maps of random walks on complex networks reveal community structure," *Proceedings of the National Academy of Sciences of the United States of America*, vol. 105, 2008.
- [12] F. McSherry, "Spectral partitioning of random graphs," in *Proceedings of the 42nd IEEE Symposium on Foundations of Computer Science*, 2001, pp. 529–537.
- [13] K. Rohe, S. Chatterjee, and B. Yu, "Spectral clustering and the high-dimensional stochastic blockmodel," *Annals of Statistics*, vol. 39, pp. 1878–1915, 2011.
- [14] D. L. Sussman, M. Tang, D. E. Fishkind, and C. E. Priebe, "A consistent adjacency spectral embedding for stochastic blockmodel graphs," *Journal of the American Statistical Association*, vol. 107, pp. 1119–1128, 2012.
- [15] U. V. Luxburg, "A tutorial on spectral clustering," *Statistics and computing*, vol. 17, pp. 395–416, 2007.
- [16] T. Qin and K. Rohe, "Regularized spectral clustering under the degree-corrected stochastic blockmodel," *Advances in Neural Information Processing Systems*, 2013.
- [17] K. Chaudhuri, F. Chung, and A. Tsiatas, "Spectral partitioning of graphs with general degrees and the extended planted partition model," in *Proceedings of the 25th conference on learning theory*, 2012.
- [18] V. Lyzinski, D. L. Sussman, M. Tang, A. Athreya, and C. E. Priebe, "Perfect clustering for stochastic blockmodel graphs via adjacency spectral embedding," *Electronic Journal of Statistics*, vol. 8, pp. 2905–2922, 2014.
- [19] E. Mossel, J. Neeman, and A. Sly, "Stochastic block models and reconstruction," *Probability Theory and Related Fields*, In press.
- [20] B. Hajek, Y. Wu, and J. Xu, "Achieving exact cluster recovery threshold via semidefinite programming," *IEEE Transactions on Information Theory*, vol. 62, pp. 2788–2797, 2016.
- [21] C. Gao, Z. Ma, A. Y. Zhang, and H. H. Zhou, "Achieving optimal misclassification proportion in stochastic blockmodel," 2015, arXiv preprint at <http://arxiv.org/abs/1505.03722>.
- [22] J. Lei and A. Rinaldo, "Consistency of spectral clustering in stochastic blockmodels," *Annals of Statistics*, vol. 43, pp. 215–237, 2015.
- [23] H. Pao, G. A. Coppersmith, and C. E. Priebe, "Statistical inference on random graphs: Comparative power analyses via Monte Carlo," *Journal of Computational and Graphical Statistics*, vol. 20, pp. 395–416, 2011.
- [24] A. Rukhin and C. E. Priebe, "A comparative power analysis of the maximum degree and size invariants for random graph inference," *Journal of Statistical Planning and Inference*, vol. 141, pp. 1041–1046, 2011.
- [25] D. Koutra, J. T. Vogelstein, and C. Faloutsos, "Delta-Con: A principled massive-graph similarity function," in *Proceedings of the SIAM International Conference in Data Mining*, 2013, pp. 162–170.
- [26] M. Rosvall and C. T. Bergstrom, "Mapping change in large networks," *PLOS ONE*, vol. 5, 2010.
- [27] D. Asta and C. R. Shalizi, "Geometric network comparison," 2014, arXiv preprint. <http://arxiv.org/abs/1411.1350>.
- [28] M. Tang, A. Athreya, D. L. Sussman, V. Lyzinski, and C. E. Priebe, "A nonparametric two-sample hypothesis for random dot product graphs," *Bernoulli*, 2016, in press.
- [29] M. Tang, A. Athreya, D. L. Sussman, V. Lyzinski, Y. Park, and C. E. Priebe, "A semiparametric two-sample hypothesis testing for random dot product graphs," *Journal of Computational and Graphical Statistics*, 2016, in press.
- [30] Y. Wang and G. Wong, "Stochastic blockmodels for

- directed graphs," *Journal of the American Statistical Association*, vol. 82, pp. 8–19, 1987.
- [31] P. W. Holland, K. Laskey, and S. Leinhardt, "Stochastic blockmodels: First steps," *Social Networks*, vol. 5, pp. 109–137, 1983.
- [32] T. P. Peixoto, "Hierarchical block structures and high-resolution model selection in large networks," *Physical Review X*, vol. 4, no. 011047, pp. 1–18, 2014.
- [33] C. L. M. Nickel, "Random dot product graphs: A model for social networks," Ph.D. dissertation, Johns Hopkins University, 2006.
- [34] P. D. Hoff, A. E. Raftery, and M. S. Handcock, "Latent space approaches to social network analysis," *Journal of the American Statistical Association*, vol. 97, pp. 1090–1098, 2002.
- [35] A. Clauset, M. E. J. Newman, and C. Moore, "Finding community structure in very large networks," *Physical Review E*, vol. 70, 2004.
- [36] M. Mariadassou, S. Robin, and C. Vacher, "Uncovering latent structure in valued graphs: A variational approach," *Annals of Applied Statistics*, vol. 4, pp. 715–742, 2010.
- [37] M. Sales-Pardo, R. Guimerà, A. A. Moreira, and L. A. N. Amaral, "Extracting the hierarchical organization of complex systems," *Proceedings of the National Academy of Sciences of the United States of America*, vol. 104, 2007.
- [38] J. Leskovec, D. Chakrabarti, J. Kleinberg, C. Faloutsos, and Z. Ghahramani, "Kronecker graphs: An approach to modeling networks," *Journal of Machine Learning Research*, vol. 11, pp. 985–1042, 2010.
- [39] Y. Park, C. Moore, and J. S. Bader, "Dynamic networks from hierarchical Bayesian graph clustering," *PLOS ONE*, vol. 5, 2010.
- [40] Y.-Y. Ahn, J. P. Bagrow, and S. Lehmann, "Link communities reveal multiscale complexity in networks," *Nature*, vol. 466, 2010.
- [41] D. L. Sussman, M. Tang, and C. E. Priebe, "Consistent latent position estimation and vertex classification for random dot product graphs," *IEEE Transactions on Pattern Analysis and Machine Intelligence*, vol. 36, pp. 48–57, 2014.
- [42] R. Vidal, "A tutorial on subspace clustering," *IEEE Signal Processing Magazine*, vol. 28, pp. 52–68, 2010.
- [43] S. Chatterjee, "Matrix estimation by universal singular value thresholding," *The Annals of Statistics*, vol. 43, pp. 177–214, 2014.
- [44] L. Kaufman and P. J. Rousseeuw, *Finding Groups in Data: An Introduction to Cluster Analysis*. John Wiley & Sons, 2009, vol. 344.
- [45] M. Zhu and A. Ghodsi, "Automatic dimensionality selection from the scree plot via the use of profile likelihood," *Computational Statistics & Data Analysis*, vol. 51, pp. 918–930, 2006.
- [46] V. Lyzinski, D. L. Sussman, D. E. Fishkind, H. Pao, L. Chen, J. T. Vogelstein, Y. Park, and C. E. Priebe, "Spectral clustering for divide-and-conquer graph matching," *Parallel Computing*, vol. 47, pp. 70–87, 2015.
- [47] A. Clauset, C. Moore, and M. E. J. Newman, "Hierarchical structure and the prediction of missing links in networks," *Nature*, vol. 453, pp. 98–101, 2008.
- [48] C. E. Priebe, D. L. Sussman, M. Tang, and J. T. Vogelstein, "Statistical inference on errorfully observed graphs," *Journal of Computational and Graphical Statistics*, vol. 24, 2015.
- [49] D. Zheng, D. Mhembere, R. Burns, J. T. Vogelstein, C. E. Priebe, and A. S. Szalay, "Flashgraph: Processing billion-node graphs on an array of commodity SSDs," in *13th USENIX Conference on File and Storage Technologies (FAST 15)*, 2015.
- [50] C. E. Priebe, D. J. Marchette, Z. Ma, and S. Adali, "Manifold matching: Joint optimization of fidelity and commensurability," *Brazilian Journal of Probability and Statistics*, vol. 27, pp. 377–400, 2013.
- [51] M. Tang, D. L. Sussman, and C. E. Priebe, "Universally consistent vertex classification for latent position graphs," *Annals of Statistics*, vol. 31, pp. 1406–1430, 2013.
- [52] G. Csardi and T. Nepusz, "The igraph software package for complex network research," *InterJournal, Complex Systems*, vol. 1695, no. 5, pp. 1–9, 2006.
- [53] G. W. Stewart and J.-G. Sun, *Matrix perturbation theory*. Academic Press, 1990.
- [54] L. Lu and X. Peng, "Spectra of edge-independent random graphs," *Electronic Journal of Combinatorics*, vol. 20, 2013.

## APPENDIX

We now provide proofs of Theorem 5 and Lemma 6. We will state and prove Theorem 5 in slightly greater generality here, by first introducing the notion of a random dot product graph with a given sparsity factor  $\rho_n$ .

**Definition 13** (The  $d$ -dimensional random dot product graph with sparsity factor  $\rho_n$ ). Let  $F$  be a distribution on a set  $\mathcal{X} \subset \mathbb{R}^d$  satisfying  $x^\top y \in [0, 1]$  for all  $x, y \in \mathcal{X}$ . We say  $(X, A) \sim \text{RDPG}(F)$  with sparsity factor  $\rho_n \leq 1$  if the following hold. Let  $X_1, \dots, X_n \sim F$  be independent random variables and define

$$X = [X_1 \mid \dots \mid X_n]^\top \in \mathbb{R}^{n \times d} \text{ and } P = \rho_n X X^\top \in [0, 1]^{n \times n}. \quad (10)$$

As before, the  $X_i$  are the latent positions for the random graph. The matrix  $A \in \{0, 1\}^{n \times n}$  is defined to be a symmetric, hollow matrix such that for all  $i < j$ , conditioned on  $X_i, X_j$  the  $A_{ij}$  are independent and

$$A_{ij} \sim \text{Bernoulli}(\rho_n X_i^\top X_j), \quad (11)$$

namely,

$$\Pr[A \mid X] = \prod_{i < j} (\rho_n X_i^\top X_j)^{A_{ij}} (1 - \rho_n X_i^\top X_j)^{(1-A_{ij})} \quad (12)$$

Recall that we denote the second moment matrix for the  $X_i$  by  $\Delta = \mathbb{E}(X_1 X_1^\top)$ , and we assume that  $\Delta$  is of rank  $d$ .

**Definition 14** (Embedding of  $A$  and  $P$ ). Suppose that  $A$  is as in Definition 13. Then our estimate for the  $\rho_n^{1/2} X$  (up to rotation) is  $\hat{X} = U_A S_A^{1/2}$ , where  $S_A \in \mathbb{R}^{d \times d}$  is the diagonal submatrix with the  $d$  largest eigenvalues (in magnitude) of  $|A|$  and  $U_A \in \mathbb{R}^{n \times d}$  is the matrix whose orthonormal columns are the corresponding eigenvectors. Similarly, we let  $U_P S_P U_P^\top$  denote the spectral decomposition of  $P$ . Note that  $P$  is of rank  $d$ .

Theorem 5 follows as an easy consequence of the more general Theorem 15, which we state below.

**Theorem 15.** *Let  $(A, X) \sim \text{RDPG}(F)$  with rank  $d$  second moment matrix and sparsity factor  $\rho_n$ . Let  $E_n$  be the event that there exists a rotation matrix  $W \in \mathbb{R}^{d \times d}$  such that*

$$\max_i \|\hat{X}_i - \rho_n^{1/2} W X_i\| \leq \frac{C d^{1/2} \log^2 n}{\sqrt{n \rho_n}}$$

where  $C > 0$  is some fixed constant. Then  $E_n$  occurs asymptotically almost surely.

### Proof of Theorem 15

The proof of Theorem 15 will follow from a succession of supporting results. We note that Theorem 18, which deals with the accuracy of spectral embedding estimates in Frobenius norm, may be of independent interest. In

what follows, for a matrix  $A \in \mathbb{R}^{m \times m}$ ,  $\|A\|$  will denote the spectral norm of  $A$ .

We begin with a short proposition.

**Proposition 16.** *Let  $(A, X) \sim \text{RDPG}(F)$  with sparsity factor  $\rho_n$ . Let  $W_1 \Sigma W_2^\top$  be the singular value decomposition of  $U_P^\top U_A$ . Then asymptotically almost surely,*

$$\|U_P^\top U_A - W_1 W_2^\top\|_F = O((n \rho_n)^{-1})$$

*Proof:* Let  $\sigma_1, \sigma_2, \dots, \sigma_d$  denote the singular values of  $U_P^\top U_A$  (the diagonal entries of  $\Sigma$ ). Then  $\sigma_i = \cos(\theta_i)$  where the  $\theta_i$  are the principal angles between the subspaces spanned by  $U_A$  and  $U_P$ . Furthermore, by the Davis-Kahan  $\sin(\Theta)$  theorem (see e.g., Theorem 3.6 in [53]),

$$\|U_A U_A^\top - U_P U_P^\top\| = \max_i |\sin(\theta_i)| \leq \frac{\|A - P\|}{\lambda_d(P)}$$

for sufficiently large  $n$ . Recall here  $\lambda_d(P)$  denotes the  $d$ -th largest eigenvalue of  $P$ . The spectral norm bound for  $A - P$  from Theorem 6 in [54] then gives

$$\|U_A U_A^\top - U_P U_P^\top\| \leq \frac{C \sqrt{n \rho_n}}{n \rho_n} = O((n \rho_n)^{-1/2}).$$

We thus have

$$\begin{aligned} \|U_P^\top U_A - W_1 W_2^\top\|_F &= \|\Sigma - I\|_F = \sqrt{\sum_{i=1}^d (1 - \sigma_i)^2} \\ &\leq \sum_{i=1}^d (1 - \sigma_i) \leq \sum_{i=1}^d (1 - \sigma_i^2) \\ &= \sum_{i=1}^d \sin^2(\theta_i) \\ &\leq d \|U_A U_A^\top - U_P U_P^\top\|_F^2 = O((n \rho_n)^{-1}) \end{aligned}$$

as desired.  $\square$

Denote by  $W^*$  the orthogonal matrix  $W_1 W_2^\top$  as defined in the above proposition. We now establish the following key lemma. The lemma allows us to exchange the order of the orthogonal transformation  $W^*$  and the diagonal scaling transformation  $S_A$  or  $S_P$ .

**Lemma 17.** *Let  $(A, X) \sim \text{RDPG}(F)$  with sparsity factor  $\rho_n$ . Then asymptotically almost surely,*

$$\|W^* S_A - S_P W^*\|_F = O(\log n)$$

and

$$\|W^* S_A^{1/2} - S_P^{1/2} W^*\|_F = O(\log n (n \rho_n)^{-1/2})$$

*Proof:* Let  $R = U_A - U_P U_P^\top U_A$ . We note that  $R$  is the residual after projecting  $U_A$  orthogonally onto the column space of  $U_P$ , and note

$$\|U_A - U_P U_P^\top U_A\|_F = O((n \rho_n)^{-1/2}).$$



We derive that

$$\begin{aligned}
W^*S_A &= (W^* - U_P^\top U_A)S_A + U_P^\top U_A S_A \\
&= (W^* - U_P^\top U_A)S_A + U_P^\top A U_A \\
&= (W^* - U_P^\top U_A)S_A + U_P^\top (A - P)U_A + U_P^\top P U_A \\
&= (W^* - U_P^\top U_A)S_A + U_P^\top (A - P)R \\
&\quad + U_P^\top (A - P)U_P U_P^\top U_A + U_P^\top P U_A \\
&= (W^* - U_P^\top U_A)S_A + U_P^\top (A - P)R \\
&\quad + U_P^\top (A - P)U_P U_P^\top U_A + S_P U_P^\top U_A
\end{aligned}$$

Writing  $S_P U_P^\top U_A = S_P (U_P^\top U_A - W^*) + S_P W^*$  and rearranging terms, we obtain

$$\begin{aligned}
\|W^*S_A - S_P W^*\|_F &\leq \|W^* - U_P^\top U_A\|_F (\|S_A\| + \|S_P\|) \\
&\quad + \|U_P^\top (A - P)R\|_F \\
&\quad + \|U_P^\top (A - P)U_P U_P^\top U_A\|_F \\
&\leq O(1) + O(1) \\
&\quad + \|U_P^\top (A - P)U_P\|_F \|U_P^\top U_A\|
\end{aligned}$$

asymptotically almost surely. Now,  $\|U_P^\top U_A\| \leq 1$ . Hence we can focus on the term  $U_P^\top (A - P)U_P$ , which is a  $d \times d$  matrix whose  $ij$ -th entry is of the form

$$\begin{aligned}
u_i^\top (A - P)u_j &= \sum_{k=1}^n \sum_{l=1}^n (A_{kl} - P_{kl})u_{ik}u_{jl} \\
&= 2 \sum_{k,l:k < l} (A_{kl} - P_{kl})u_{ik}u_{jl} - \sum_k P_{kk}u_{ik}u_{jk}
\end{aligned}$$

where  $u_i$  and  $u_j$  are the  $i$ -th and  $j$ -th columns of  $U_P$ . Thus, conditioned on  $P$ ,  $u_i^\top (A - P)u_j$  is a sum of independent mean 0 random variables and a term of order  $O(1)$ . Now, by Hoeffding's inequality,

$$\begin{aligned}
&\mathbb{P} \left[ \left| \sum_{k,l:k < l} 2(A_{kl} - P_{kl})u_{ik}u_{jl} \right| \geq t \right] \\
&\leq 2 \exp \left( \frac{-2t^2}{\sum_{k,l:k < l} (2u_{ik}u_{jl})^2} \right) \leq 2 \exp(-t^2).
\end{aligned}$$

Therefore, each entry of  $U_P^\top (A - P)U_P$  is of order  $O(\log n)$  asymptotically almost surely, and as a consequence,

$$\|U_P^\top (A - P)U_P\|_F$$

is of order  $O(\log n)$  asymptotically almost surely. Hence,

$$\|W^*S_A - S_P W^*\| = O(\log n)$$

asymptotically almost surely. We establish  $\|W^*S_A^{1/2} - S_P^{1/2}W^*\|_F = O(\log n(n\rho_n)^{-1/2})$  by noting that the  $ij$ -th entry of  $W^*S_A^{1/2} - S_P^{1/2}W^*$  can be written as

$$W_{ij}^* (\lambda_i^{1/2}(A) - \lambda_j^{1/2}(P)) = W_{ij}^* \frac{\lambda_i(A) - \lambda_j(P)}{\lambda_i^{1/2}(A) + \lambda_j^{1/2}(P)}$$

and that the eigenvalues  $\lambda_i^{1/2}(A)$  and  $\lambda_j^{1/2}(P)$  are all of order  $\Omega(\sqrt{n\rho_n})$  (see [41]).  $\square$

We next present Theorem 18, which extends earlier results on Frobenius norm accuracy of the adjacency spectral embedding from [18] even when the second moment matrix  $\mathbb{E}[X_1 X_1^\top]$  does not have distinct eigenvalues.

**Theorem 18.** *Let  $(A, X) \sim \text{RDPG}(F)$  with sparsity factor  $\rho_n$ . Let  $E_n$  be the event that there exists a rotation matrix  $W$  such that*

$$\begin{aligned}
&\|\hat{X} - \rho_n^{1/2} X W\|_F \\
&= \|(A - P)U_P S_P^{-1/2}\|_F + O(\log(n)(n\rho_n)^{-1/2})
\end{aligned}$$

Then  $E_n$  occurs asymptotically almost surely.

*Proof:* Let

$$\begin{aligned}
R_1 &= U_P U_P^\top U_A - U_P W^* \\
R_2 &= (W^* S_A^{1/2} - S_P^{1/2} W^*).
\end{aligned}$$

We deduce that

$$\begin{aligned}
\hat{X} - U_P S_P^{1/2} W^* &= U_A S_A^{1/2} - U_P W^* S_A^{1/2} \\
&\quad + U_P (W^* S_A^{1/2} - S_P^{1/2} W^*) \\
&= (U_A - U_P U_P^\top U_A) S_A^{1/2} \\
&\quad + R_1 S_A^{1/2} + U_P R_2 \\
&= U_A S_A^{1/2} - U_P U_P^\top U_A S_A^{1/2} \\
&\quad + R_1 S_A^{1/2} + U_A R_2
\end{aligned}$$

Now,  $U_P U_P^\top P = P$  and  $U_A S_A^{1/2} = A U_A S_A^{-1/2}$ . Hence

$$\begin{aligned}
\hat{X} - U_P S_P^{1/2} W^* &= (A - P)U_A S_A^{-1/2} \\
&\quad - U_P U_P^\top (A - P)U_A S_A^{-1/2} \\
&\quad + R_1 S_A^{1/2} + U_A R_2
\end{aligned}$$

Writing

$$\begin{aligned}
R_3 &= U_A - U_P W^* \\
&= U_A - U_P U_P^\top U_A + R_1,
\end{aligned}$$

we derive that

$$\begin{aligned}
\hat{X} - U_P S_P^{1/2} W^* &= (A - P)U_P W^* S_A^{-1/2} \\
&\quad - U_P U_P^\top (A - P)U_P W^* S_A^{-1/2} \\
&\quad + (I - U_P U_P^\top)(A - P)R_3 S_A^{-1/2} \\
&\quad + R_1 S_A^{1/2} + U_A R_2
\end{aligned}$$

Now

$$\begin{aligned}
\|R_1\|_F &= O((n\rho_n)^{-1}), \\
\|R_2\|_F &= O(\log n(n\rho_n)^{-1/2}), \text{ and} \\
\|R_3\|_F &= O((n\rho_n)^{-1/2});
\end{aligned}$$

indeed, we recall

$$\|U_A - U_P U_P^\top U_A\|_F = O((n\rho_n)^{-1/2}).$$

Furthermore, Hoeffding's inequality guarantees that

$$\begin{aligned}
&\|U_P U_P^\top (A - P)U_P W^* S_A^{-1/2}\|_F \\
&\leq \|U_P^\top (A - P)U_P\|_F \|S_A^{-1/2}\|_F = O(\log n(n\rho_n)^{-1/2})
\end{aligned}$$

As a consequence,

$$\begin{aligned} & \|\hat{X} - U_P S_P^{1/2} W^*\|_F \\ &= \|(A - P)U_P W^* S_A^{-1/2}\|_F + O(\log n(n\rho_n)^{-1/2}) \\ &= \|(A - P)U_P S_P^{-1/2} W^* \\ &\quad + (A - P)U_P (S_P^{-1/2} W^* - W^* S_A^{-1/2})\|_F \\ &\quad + O(\log n(n\rho_n)^{-1/2}) \end{aligned}$$

Using a very similar argument as that employed in the proof of Lemma 17, we can show that

$$\|S_P^{-1/2} W^* - W^* S_A^{-1/2}\|_F = O(\log n(n\rho_n)^{-3/2})$$

Recall that

$$\begin{aligned} & \|((A - P)U_P (S_P^{-1/2} W^* - W^* S_A^{-1/2}))\|_F \\ & \leq \|(A - P)U_P\| \| (S_P^{-1/2} W^* - W^* S_A^{-1/2}) \|_F \end{aligned}$$

Further, as already mentioned, Theorem 6 of [54] ensures that  $\|(A - P)\|$  is of order  $O(\sqrt{n\rho_n})$  asymptotically almost surely; this implies, of course, identical bounds on  $\|(A - P)U_P\|$ . We conclude that

$$\begin{aligned} & \|\hat{X} - U_P S_P^{1/2} W^*\|_F \\ &= \|(A - P)U_P S_P^{-1/2} W^*\|_F + O(\log(n)(n\rho_n)^{-1/2}) \\ &= \|(A - P)U_P S_P^{-1/2}\|_F + O(\log(n)(n\rho_n)^{-1/2}). \quad (13) \end{aligned}$$

Finally, to complete the proof, we note that

$$\rho_n^{1/2} X = U_P S_P^{1/2} W$$

for some orthogonal matrix  $W$ . Since  $W^*$  is also orthogonal, we conclude that there exists some orthogonal  $\tilde{W}$  for which

$$\rho_n^{1/2} X \tilde{W} = U_P S_P^{1/2} W^*,$$

as desired.  $\square$

We are now ready to prove Theorem 15.

*Proof:* To establish Theorem 15, we begin by noting that

$$\begin{aligned} \|\hat{X} - \rho_n^{1/2} X W\|_F &= \|(A - P)U_P S_P^{-1/2}\|_F \\ &\quad + O(\log(n)(n\rho_n)^{-1/2}) \end{aligned}$$

and hence

$$\begin{aligned} & \max_i \|\hat{X}_i - \rho_n^{1/2} W X_i\| \\ & \leq \frac{1}{\lambda_d^{1/2}(P)} \max_i \|((A - P)U_P)_i\| + O(\log(n)(n\rho_n)^{-1/2}) \\ & \leq \frac{d^{1/2}}{\lambda_d^{1/2}(P)} \max_j \|(A - P)u_j\|_\infty + O(\log(n)(n\rho_n)^{-1/2}) \end{aligned}$$

where  $u_j$  denotes the  $j$ -th column of  $U_P$ . Now, for a given  $j$  and a given index  $i$ , the  $i$ -th element of the vector  $(A - P)u_j$  is of the form

$$\sum_k (A_{ik} - P_{ik})u_{jk}$$

and once again, by Hoeffding's inequality, the above term is  $O(\log n)$  asymptotically almost surely. Taking the union bound over all indices  $i$  and all columns  $j$  of  $U_P$ , we conclude

$$\begin{aligned} \max_i \|\hat{X}_i - \rho_n^{1/2} W X_i\| & \leq \frac{C d^{1/2}}{\lambda_d^{1/2}(P)} \log^2(n) \\ & \quad + O(\log(n)(n\rho_n)^{-1/2}) \\ & \leq \frac{C d^{1/2} \log^2 n}{\sqrt{n\rho_n}} \end{aligned}$$

as desired.  $\square$

## Proof of Lemma 6

Our assumption that  $p < q$ , and Theorem 5, gives that

$$\hat{p} := \max_{i,j:i \neq j} \max_{\ell,h} \langle \hat{\xi}_i^{(2)}(\ell, \cdot), \hat{\xi}_j^{(2)}(h, \cdot) \rangle,$$

and

$$\hat{q} := \min_i \min_{\ell,h} \langle \hat{\xi}_i^{(2)}(\ell, \cdot), \hat{\xi}_i^{(2)}(h, \cdot) \rangle,$$

are such that  $\hat{p} < \hat{q}$  asymptotically almost surely. The proof of Lemma 6 follows from the following proposition and the fact that  $\hat{p} < \hat{q}$  asymptotically almost surely.

**Proposition 19.** *Given the assumptions of Lemma 6 and Lemma 5, let  $E_n$  be the event that the set  $\mathcal{S}_n$  obtained in Algorithm 2 satisfies*

$$|\mathcal{S}_n \cap \{\hat{\xi}_i^{(2)}(\ell, \cdot)\}_{\ell=1}^{|V(H_i)|}| = 1$$

for all  $i \in [R]$ . Then  $E_n$  occurs asymptotically almost surely.

*Proof:* For each  $i \in [R]$ , define  $C_j = \{\hat{\xi}_i^{(2)}(\ell, \cdot)\}_{\ell=1}^{|V(H_i)|}$ . The proposition follows immediately from proving

- (1) For all  $i \in [n]$ , if  $\hat{X}(i, \cdot)$  belongs to  $C_j$  and  $|\mathcal{S}_{i-1} \cap C_j| = 0$ , then  $\hat{X}(i, \cdot)$  will be added to  $\mathcal{S}_{i-1}$ .
- (2) For all  $i \in [n]$ , if  $s \in \mathcal{S}_{i-1}$  belongs to  $C_j$  and  $|\mathcal{S}_{i-1} \cap C_j| = 1$ , then  $s \in \mathcal{S}_i$  (i.e.,  $s$  will not be removed from  $\mathcal{S}_{i-1}$ ).

For (1), for fixed  $i \in [n]$ , if  $\hat{X}(i, \cdot)$  belongs to  $C_j$  and  $|\mathcal{S}_{i-1} \cap C_j| = 0$ , then

$$\max_{s \in \mathcal{S}_{i-1}} \langle \hat{X}(i, \cdot), s \rangle \leq \hat{p}.$$

By the pigeonhole principle, there exist  $y, z \in \mathcal{S}_{i-1}$  such that  $y, z \in C_k$  for some  $k \in [R]$ ,  $k \neq j$ . Thus  $\langle y, z \rangle \geq \hat{q}$ , and

$$\max_{s \in \mathcal{S}_{i-1}} \langle \hat{X}(i, \cdot), s \rangle < \max_{x, w \in \mathcal{S}_{i-1}} \langle x, w \rangle,$$

and hence  $\hat{X}(i, \cdot)$  will be added to  $\mathcal{S}_{i-1}$ .

For (2), for fixed  $i \in [n]$ , suppose  $s \in \mathcal{S}_{i-1}$  belongs to  $C_j$  and  $|\mathcal{S}_{i-1} \cap C_j| = 1$ . Consider two cases. First, suppose that for each  $k \in [R]$ ,  $|\mathcal{S}_{i-1} \cap C_k| = 1$ . Then

$$\max_{s \in \mathcal{S}_{i-1}} \langle \hat{X}(i, \cdot), s \rangle \geq \hat{q} > \hat{p} > \max_{x, w \in \mathcal{S}_{i-1}} \langle x, w \rangle,$$

and  $\widehat{X}(i, \cdot)$  will not be added to  $\mathcal{S}_{i-1}$ , and so  $s \in \mathcal{S}_i$ . Otherwise, there exists  $y, z \in \mathcal{S}_{i-1}$  satisfying  $y, z \in C_k$  for some  $k \in [R]$ ,  $k \neq j$ . Therefore

$$\max_{x \in \mathcal{S}_{i-1}} \langle x, s \rangle \leq \hat{p} < \hat{q} \leq \langle y, z \rangle \leq \max_{x, w \in \mathcal{S}_{i-1}} \langle x, w \rangle,$$

and even if  $\widehat{X}(i, \cdot)$  is added to  $\mathcal{S}_{i-1}$ , then  $s$  will not be removed from  $\mathcal{S}_{i-1}$ , as desired.  $\square$

To finish the proof of Lemma 6, from Proposition 19, the set  $S_n$  will contain a single row of  $\widehat{\xi}^{(j)}$  for each  $j \in [R]$  asymptotically almost surely. For each  $i \in [n]$ , if  $\widehat{X}(i, \cdot) \in C_k$ , then asymptotically almost surely

$$\operatorname{argmax}_j \langle \widehat{X}(i, \cdot), s_j \rangle \in C_k,$$

as desired.